Contract No:

This document was prepared in conjunction with work accomplished under Contract No. DE-AC09-08SR22470 with the U.S. Department of Energy (DOE) Office of Environmental Management (EM).

Disclaimer:

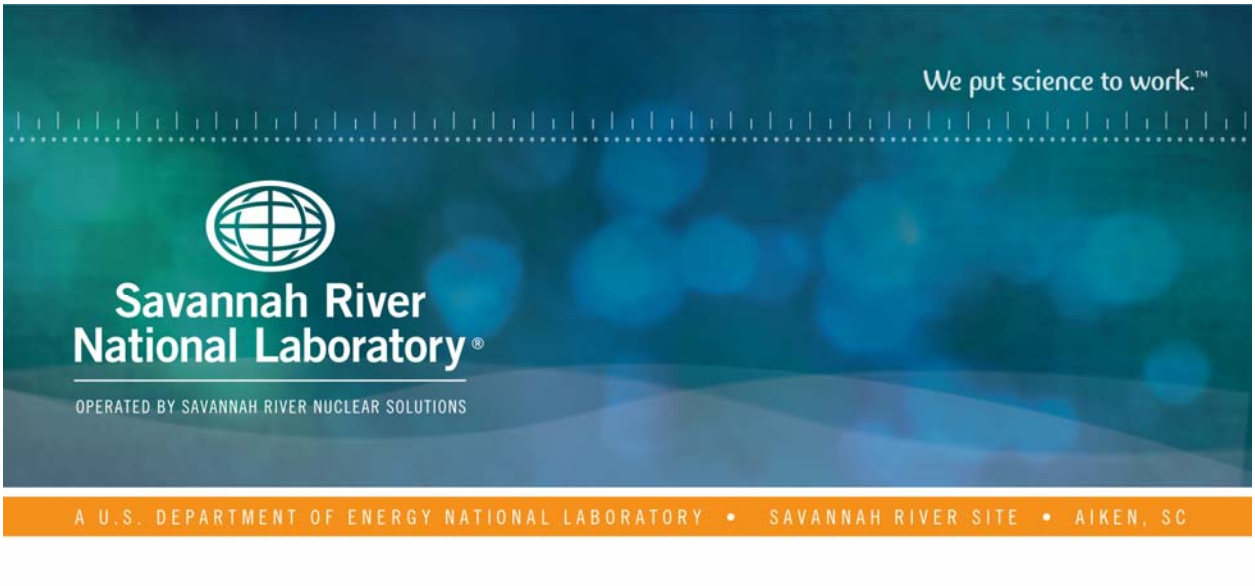

Thermolytic Hydrogen Generation Testing of Tank 22 Material

C.J. Martino, J.M. Pareizs, and J.D. Newell

November 2018

SRNL-STI-2018-00385, Revision 0

DISCLAIMER

Printed in the United States of America

Prepared for
U.S. Department of Energy

SRNL-STI-2018-00385
Revision 0

Keywords: *DWPF Recycle, Alternate Reductant, Tank Farm*

Retention: *Permanent*

Thermolytic Hydrogen Generation Testing of Tank 22 Material

C.J. Martino
J.M. Pareizs
J.D. Newell

November 2018

Prepared for the U.S. Department of Energy under contract number DE-AC09-08SR22470.

Savannah River National Laboratory™
OPERATED BY SAVANNAH RIVER NUCLEAR SOLUTIONS

REVIEWS AND APPROVALS

AUTHORS:

_____
C.J. Martino, Process Technology Programs Date

_____
J.M. Pareizs, Process Technology Programs Date

_____
J.D. Newell, Process Technology Programs Date

TECHNICAL REVIEW:

_____
C.L. Crawford, Advanced Characterization and Processing Date

APPROVAL:

_____
F.M. Pennebaker, Program Manager, Chemical Processing Technologies Date

_____
S.D. Fink, Director, Chemical Processing Technologies Date

_____
J.E. Occhipinti, Manager, Tank Farm Facility Engineering Date

EXECUTIVE SUMMARY

Savannah River National Laboratory performed hydrogen generation rate (HGR) testing using Tank 22 actual-waste sample material. The main objective of the testing was to determine the thermolysis HGR for Tank 22 material with and without added glycolate. An important use of the data from actual-waste sample testing is to validate equations for the Savannah River Site Concentration, Storage, and Transfer Facility (CSTF) HGR being developed through simulated-waste testing. Not exclusive to providing data for model validation, the desired outcome of this testing was to demonstrate a negligible thermolytic HGR in Tank 22 from the contribution of glycolate from the future Defense Waste Processing Facility (DWPF) Nitric-Glycolic Acid (NGA) flowsheet to Tank 22. Tank 22 is the pathway for glycolate in the DWPF recycle stream to enter the CSTF. Testing with added glycolate used the estimated future concentration of glycolate based on DWPF recycle with limited Sludge Receipt and Adjustment Tank and Slurry Mix Evaporator (SME) material carry-over but without glycolate mitigation in the Recycle Collection Tank. Minor objectives include the determination of the impact of the glycolate source used in testing and the inclusion of sludge solids in testing.

Four HGR tests were performed using separate 1-L aliquots from mixtures (a sample supernate composite and a sample slurry aliquot) made from three Tank 22 slurry samples taken in 2016 and 2017. The four tests were as follows:

- Tank 22 sample supernate with no glycolate added,
- Tank 22 sample supernate with 120 mg/L glycolate added as sodium glycolate,
- Tank 22 sample supernate with 120 mg/L glycolate added as pH adjusted SME product supernate from previous Nitric-Glycolic Acid flowsheet qualification testing, and
- Tank 22 sample slurry with glycolate added as sodium glycolate.

The test consisted of mixing and heating the material, flowing a purge gas of known concentration over the material, condensing water from gas stream exiting the system, and measuring the concentration of hydrogen and other gasses in non-condensable stream. Each HGR test consisted of a series of isothermal tests with increasing temperatures: 30 °C, 60 °C, 80 °C, and the atmospheric pressure boiling point (101.2 to 101.6 °C).

The majority of the test conditions for the Tank 22 supernate HGR measurements gave results below the limit of quantification for HGR of 5.6×10^{-8} ft^3 h^{-1} gal^{-1}. The introduction of glycolate into Tank 22 supernate at 120 mg/L both from reagent sodium glycolate and from adjusted SME product did not increase the HGR at boiling temperatures. Testing with Tank 22 slurry resulted in measurable HGR at all temperatures that ranged from of 1.61×10^{-7} ft^3 h^{-1} gal^{-1} to 2.17×10^{-7} ft^3 h^{-1} gal^{-1}. The majority of the HGR measured in the Tank 22 slurry testing is consistent with radiolytic hydrogen generation due to the presence of sludge solids.

TABLE OF CONTENTS

LIST OF TABLES

LIST OF FIGURES

LIST OF ABBREVIATIONS

ADP	Antifoam Degradation Products
CI	Confidence Interval
CPC	Chemical Processing Cell
CSTF	Concentration, Storage, and Transfer Facility
CVAA	Cold Vapor Atomic Absorption
DWPF	Defense Waste Processing Facility
DAC	Data Acquisition and Control
DSA	Documented Safety Analysis
EPA	Environmental Protection Agency
GC	Gas Chromatograph
GCCVAFS	Gas Chromatography Cold-Vapor Atomic Fluorescence Spectroscopy
HGR	Hydrogen Generation Rate
HMDSO	hexamethyldisiloxane
ICA	Ion Chromatography for Anions
ICP-ES	Inductively Coupled Plasma – Atomic Emissions Spectroscopy
ICP-MS	Inductively Coupled Plasma – Mass Spectroscopy
KM	Kaplan-Meier
LOD	Limit of Detection
LOQ	Limit of Quantification
LTAD	Low Temperature Aluminum Dissolution
NGA	Nitric-Glycolic Acid
NFA	Nitric-Formic Acid
OGCT	Off-Gas Condensate Tank
PID	Proportional-Integral-Derivative
PISA	Potential Inadequacy in the Safety Analysis
ppmv	Parts per million volume
RCT	Recycle Collection Tank
sccm	Standard cubic centimeters
SME	Slurry Mix Evaporator
SMECT	Slurry Mix Evaporator Condensate Tank
SRAT	Sludge Receipt and Adjustment Tank
SRNL	Savannah River National Laboratory
SRS	Savannah River Site
SVOA	Semi-Volatile Organics Analysis
TIC	Total Inorganic Carbon
TMS	trimethylsilanol
TOC	Total Organic Carbon
TTQAP	Task Technical and Quality Assurance Plan
TTR	Technical Task Request
UCL	Upper Confidence Limit
VOA	Volatile Organics Analysis
WTP	Waste Treatment Plant

1.0 Introduction

1.1 Background

With the implementation of the Nitric-Glycolic Acid (NGA) flowsheet at the Defense Waste Processing Facility (DWPF), small amounts of glycolate will be transferred into the Savannah River Site (SRS) Concentration, Storage, and Transfer Facility (CSTF) from the DWPF recycle stream. A literature survey indicated that glycolate sent back to the CSTF can produce hydrogen via thermolytic reactions.[1] Work performed for Hanford Reservation tank waste programs indicated that glycolate decomposition in high pH solutions containing soluble aluminum generates hydrogen.[2-3] The expected impact of glycolate on radiolytic and thermolytic hydrogen generation in the SRS CSTF and DWPF was developed.[4]

To support resolution of the Potential Inadequacy in the Safety Analysis (PISA) for the SRS CSTF,[5] Savannah River National Laboratory (SRNL) previously conducted research to determine the thermolytic hydrogen generation rate (HGR) with simulated and actual waste. Gas chromatography methods were developed and used with air-purged flow systems to quantify hydrogen generation from heated simulated and actual waste at rates applicable to the CSTF Documented Safety Analysis (DSA). Testing included a measurement of HGR on actual SRS tank waste from Tank 38 and simulated waste with the most common SRS CSTF organics at temperatures up to 140 °C.[9] This measurement with Tank 22 samples extends the knowledge from the previous sample measurements and supports current simulant testing for developing an equation for CSTF HGR with and without added glycolate.

The specific goals for Tank 22 testing included understanding HGR impacts of DWPF recycle at reasonable glycolate concentrations. After initial simulant testing with glycolate, Savannah River Remediation (SRR) personnel requested that subsequent HGR testing be performed at typical glycolate concentrations in recycle for future DWPF processing rather than unrealistically bounding levels of glycolate in the DWPF recycle stream.[6] Tank 22 is also a location where organics in the DWPF recycle stream such as Antifoam Degradation Products (ADPs) can enter the CSTF. As the typical receipt tank for the DWPF recycle stream back to the CSTF, Tank 22 supernate has a lower overall salt concentration than most other CSTF supernates. Secondary goals of the Tank 22 HGR measurements include the determination if the form of glycolate is important or if sludge solids are important to thermolytic HGR.

Further understanding of how glycolate would impact thermolytic hydrogen generation in the SRS Liquid Waste System at varying concentrations and temperatures is warranted. Additionally, improved quantification of thermolytic hydrogen generation in the SRS Liquid Waste System in the absence of glycolate is desired. To address these needs, SRR issued a Technical Task Request (TTR) requesting that SRNL perform simulant and actual waste testing to support thermolysis HGR determination for Tank Farm processes.[7] This report covers a portion of the data that is being gathered as Task 2 of the TTR, specifically gathering actual waste data to support actual waste spiked with glycolate. A Task Technical and Quality Assurance Plan (TTQAP) further defines the actual-waste and simulated-waste testing.[8] Finally, a Run Plan gives test details specific to the HGR testing of Tank 22 actual waste samples.[6] As specified by the TTR and TTQAP and as detailed in the Run Plan, a basis for glycolate concentration was developed for use in Tank 22 testing and subsequent testing was performed in the flow system which was deemed most appropriate for use with these samples.

1.2 Thermolytic Hydrogen Generation

A background of thermolytic hydrogen generation applicable to current CSTF organic compounds and future additions of glycolate are detailed elsewhere.[4, 9] Thermolytic HGR is summarized again here.

Thermolytic production of hydrogen from organic compounds was also described by Hu in 2004.[10] In work designed to support flammability calculations at the Hanford Waste Treatment Plant (WTP), Hu developed an empirical model describing the thermolytic production of H_2 from organic molecules as a function of temperature, organic carbon content, and aluminum content. This model is given in Equation 1:

$$HGR_{thm} = a_{thm} \cdot r_f \cdot [TOC] \cdot [Al]^{0.4} \cdot L_f \cdot e^{-E_{thm}/RT} \quad \text{Equation 1}$$

where,

HGR_{thm} = thermolytic hydrogen generation rate, mo1e kg^{-1} day^{-1}
a_{thm} = pre-exponential factor, 3.94×10^9 mo1 kg^{-1} day^{-1}
r_f = reactivity coefficient
$[TOC]$ = concentration of total organic carbon in the liquid, wt%
$[Al]$ = concentration of aluminum, wt%
L_f = mass fraction of waste present as liquid
E_{thm} = thermolytic activation energy, 89,600 J $mole^{-1}$
R = gas constant, 8.314 J $mole^{-1}$ K^{-1}
T = temperature, K

Both the activation energy and the pre-exponential factor are values regressed from hydrogen generation measurements specific to Hanford actual waste samples at temperatures between 60 and 120 °C. Thus, the values are representative of the specific blend of organics present in that waste. The reactivity factor was used to improve the fit of the data, with recommended values varying between 0.15 and 1. Data generated in this report is compared to the most conservative recommendation, using Equation 1 and a value of reactivity factor of $r_f = 1$. Note that the use of a reactivity factor equal to 1 is more conservative than the values recommended by Hu for Hanford waste tanks (0.3 or 0.6).

The advantage of the empirical model developed by Hu is that exact knowledge of the concentrations for each organic species present is not needed. Rather, a composite measurement (i.e., Total Organic Carbon, TOC) is employed such that hydrogen generation from organic thermolysis can be predicted within a factor of 3 for Hanford organics without the need for extensive sampling and characterization campaigns. This approach is especially useful in the context of evaluating SRS wastes, where hundreds of organics are known to exist in trace amounts.[11]

In 2017, Crawford and King used observations and data generated by Ashby to develop a rate expression for hydrogen generation due to glycolate thermolysis.[4] This rate equation was generated by assuming that the rate of destruction of glycolate is the maximum H_2 production rate (i.e., one mole of glycolate can make one mole of hydrogen). Using this assumption, Ashby's kinetic data for glycolate degradation, and an observed hydrogen generation activation energy (113,000 J/mol), a rate expression derived from the Crawford and King model can be developed, given in Equation 2:

$$HGR_{thm}^{gly} = k\frac{[Al]\left[NO_2^-\right][gly]}{\left[OH^-\right]} e^{\frac{-E_A}{R}\left(\frac{1}{T}-\frac{1}{393.15}\right)} \quad \text{Equation 2}$$

where,

HGR_{thm}^{gly} = rate of hydrogen production by glycolate thermolysis, moles L^{-1} h^{-1}
k = rate constant for glycolate degradation at 120 °C, 4×10^{-4} L mol^{-1} h^{-1}

$[Al]$ = aluminum concentration, M
$[NO_2^-]$ = nitrite concentration, M
$[gly]$ = glycolate concentration, M
$[OH^-]$ = hydroxide concentration, M
E_A = activation energy for hydrogen generation, 113,000 J mol^{-1}
R = gas constant, 8.314 J mol^{-1} K^{-1}
T = temperature, K

The analyses and kinetic studies performed by Ashby comprise a matrix of tests to validate and benchmark simulant experimental data generated at SRNL.

There are significant differences between the solution compositions used by Hu and SRS waste. Similar differences exist between the experiments performed by Ashby and SRS waste. Among these deviations, aluminum concentration differences may have the greatest influence on application of the equations given the relationship described by both Hu and Ashby between HGR and soluble aluminum concentration. Simulant work to gather information more appropriate to SRS CSTF conditions is underway.[8, 12]

1.3 Glycolate Concentration Applicable to Tank 22 Testing

The Run Plan details the approach for estimating the future typical glycolate concentration.[6] The scope of Tank 22 sample testing of thermolytic HGR was to use an amount of glycolate typical (rather than bounding) of the glycolate concentration expected to be fed from DWPF to Tank 22. Specifically, historic larger carry-over (i.e., foam-over) of Sludge Receipt and Adjustment Tank (SRAT) and Slurry Mix Evaporator (SME) material into the Slurry Mix Evaporator Condensate Tank (SMECT) was considered a process upset and not included in this estimate of 'nominal' glycolate concentration. For this analysis, a larger-than-typical amount of carry-over is defined as samples having iron concentrations of 500 mg/kg or greater.

Glycolate sent to the CSTF from the DWPF using the NGA flowsheet will be sent from the Recycle Collection Tank (RCT). For the NGA flowsheet, there are two major feeds to the RCT that may contain glycolate: the SMECT and the Melter Off-Gas Condensate Tank (OGCT).

The general approach to estimating the future typical glycolate concentration was as follows:

- Examined the historic TOC measurements in the RCT and SMECT from the Nitric-Formic Acid (NFA) flowsheet,
- Excluded historic DWPF Laboratory TOC measurements where major carry-over process upset events appear to have occurred,
- Assumed that the entirety of the historic DWPF Laboratory TOC measurements are formate,
- Predicted the future glycolate concentration in the RCT based on the historic formate concentration, and
- Used SRNL laboratory-scale testing results for the NGA flowsheet to support this prediction.

As described in detail in the Run Plan,[6] historic TOC data from the NFA flowsheet.[13-15] was extended to NGA processing. A Kaplan-Meier (KM) statistical analysis was performed to estimate the average TOC in the SMECT, OGCT, and RCT for typical operation given the significant fraction of results that were non-detects. The mean TOC value was 38.0 mg C/kg with a standard deviation of 32.0 mg C/kg. Using Student's t statistic, the 95% Upper Confidence Limit (UCL) on the average TOC value was 48.3 mg C/kg. All the TOC in the RCT is conservatively assumed to be formate, which at the 95% KM UCL for TOC equals

181 mg/kg formate. The assumption that all the TOC is formate introduces a modest additional level of conservatism, since a portion of the TOC in the RCT is almost certainly antifoam, antifoam degradation products, and other organic acid anions. Based on Chemical Process Cell (CPC) testing, the glycolate concentration in the CPC and melter would be 65% of the historic formate concentration. Extending this to the RCT, the expected future glycolate concentration in the RCT is estimated to be 120 mg/L.

Assumptions used in this analysis were backed by SRNL testing of the Chemical Process Cell (CPC) and melter with the NGA flowsheet.[6] Although there is conservatism in the basis of this value, this value is not bounding of all possible transfers from DWPF to Tank 22.

The main conservatisms in using 120 mg/L glycolate include:

- Uses the 95% UCL of the historic TOC data as a basis (rather than the average by the same approach),
- Assumes all TOC in the historic data is formate,
- Assumes relationship of future glycolate to past formate is based on relative concentrations in SRAT and SME rather than relative vapor pressures, and
- Bounds laboratory-scale testing results from simulant and actual waste CPC tests.

The main non-conservatisms in testing with 120 mg/L glycolate include:

- Excludes historic large carry-over process upset events in the SMECT, and
- Assumes similar condensate (OGCT and SMECT) composition between SRNL laboratory-scale testing and actual DWPF processing for the NGA flowsheet.

2.0 Experimental

2.1 Flow System Setup

2.1.1 Shielded Cells HGR Test Apparatus

The apparatus used for thermolytic HGR testing in the Shielded Cells was based on the simulant testing flow system being used for Task 1 of the TTR and TTQAP.[7-8] The apparatus combined design elements from equipment used for previous one liter and four liter sludge batch qualification CPC testing.[16-17] The vessel holding the radioactive waste sample and the sealing lid assuring capture of gases during testing was made of Teflon®, with a volume of approximately 1.2 liters. Use of a flow-through system with minimal headspace is consistent with the HGR measurement apparatus recommended and developed for qualification of radioactive-waste feeds at the Hanford WTP.[18-19] The WTP system, however, utilizes a water-blanketed borosilicate glass vessel for holding and heating the waste (as opposed to the rod-heated Teflon® vessel), and has a significantly smaller waste sample capacity, nominally 100 mL. Teflon® fluoropolymer was chosen for HGR measurements with the flow system based on recommendations from simulant testing.[12] Teflon® was used to minimize potential interferences from performing tests in glass or stainless-steel vessels.

Apart from the Teflon® vessel, the overall experimental system used for these tests was the same as that used for the high caustic Low Temperature Aluminum Dissolution (LTAD) tests.[20] Figure 2-1 contains two photographs of the HGR measurement system. The photograph on the left is the system with the stainless-steel pot prior to its use in the LTAD tests. The photograph on the right is the same system but with a Teflon® pot installed in SRNL Shielded Cells, A Block Cell 2.

Heating was provided using two 0.375-inch diameter Alloy 800 heating rods powered by an automated direct current power supply (TDK-Lambda Genesys, GEN150-10). Mixing was controlled using a mixer

system consisting of a Servodyne mixing head coupled to an agitator shaft via a Parr high torque magnetic drive. Two 1-inch diameter, 4-blade, 45° pitched turbine stainless steel impellers were welded to the stainless-steel agitator shaft. The slurry was continually stirred over the course of the testing. Purge gas was controlled using an MKS Model 647 Multi Gas Controller and MKS Model 1179 Flow Controller. An offgas condenser allowed condensate to reflux back into the pot containing the sample material. Non-condensable gas exiting the condenser was sampled by a dedicated Agilent 3000A dual column micro gas chromatograph (GC), as described in further detail in a later subsection. A schematic depicting integration of the primary components of the HGR measurement flow system apparatus is given in Figure 2-2.

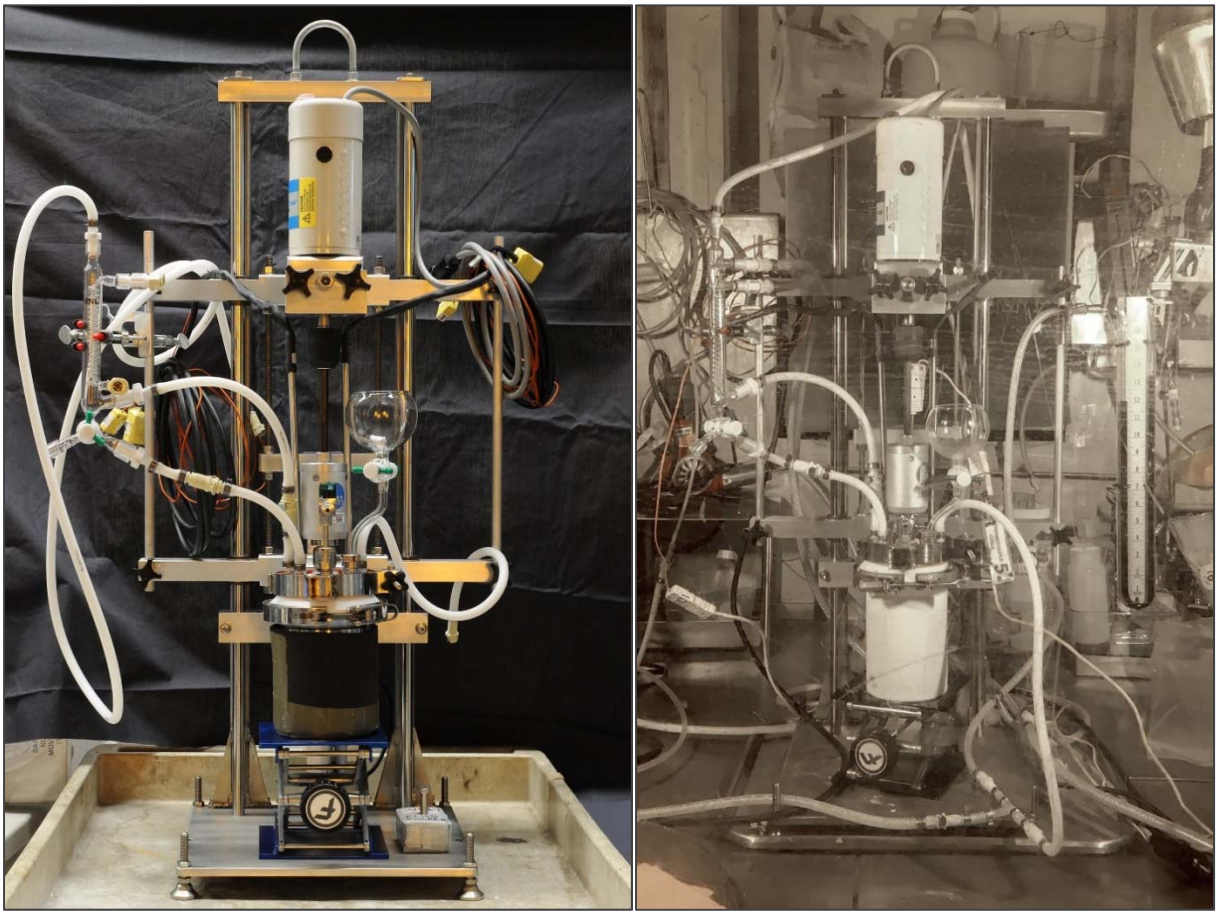

Figure 2-1. HGR test apparatus prepared for installation prior to LTAD testing (left) and in operation in during Tank 22 testing (right).

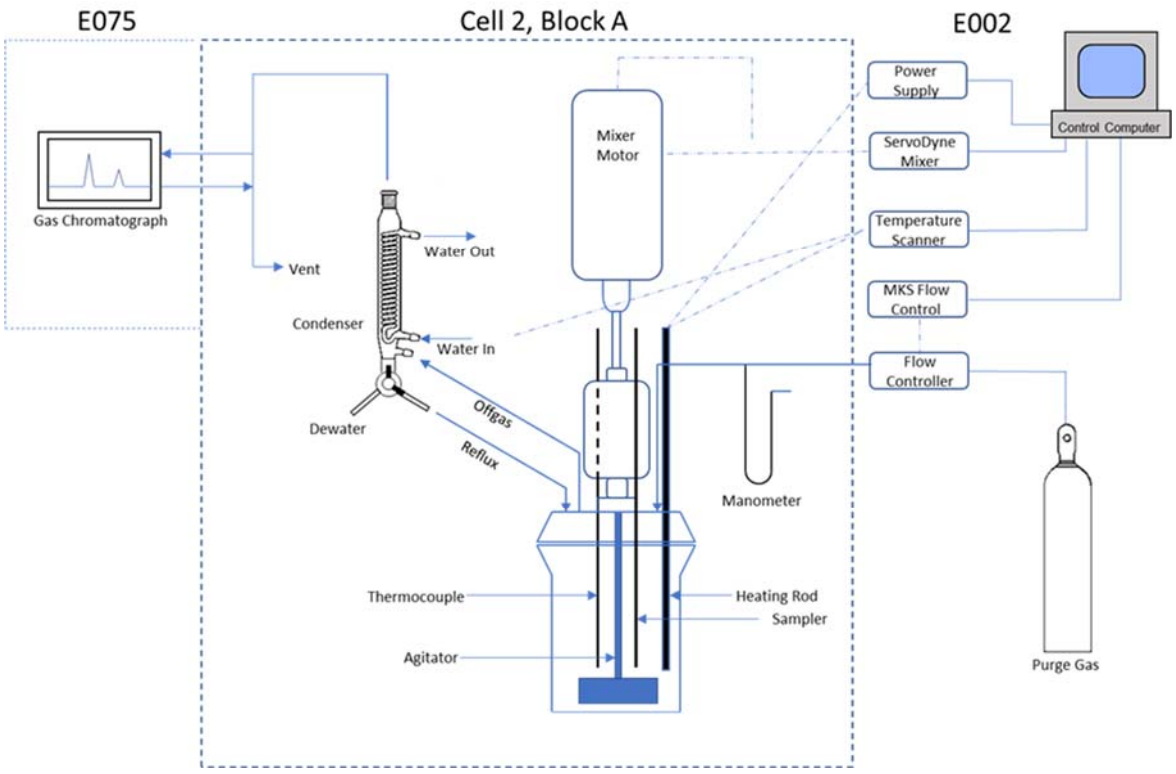

Figure 2-2. HGR Measurement Flow System Apparatus used in Tank 22 Testing.

2.1.2 Data Acquisition and Control

A Data Acquisition and Control (DAC) application was programmed using National Instruments LabVIEW software. The software that controlled the process parameters for the Tank 22 tests was the control software used for the other recent HGR measurement testing (Tank 38 and LTAD) that was originally developed for DWPF CPC flowsheet and qualification testing. The DAC logged process data and controlled mixing speed, purge gas flow rate, and heating rod temperature. A proportional-integral-derivative (PID) control algorithm governs the amount of power supplied to the heating rods by comparing the bulk process temperature to the process temperature setpoint. To prevent the rods from overheating, a control limit is defined ("rod dT limit") that prevents the heating rods from exceeding the bulk temperature by the specified amount. Given that HGR is expected to be temperature dependent, efforts were made to eliminate localized hot regions in the process vessel by minimizing the differential temperature between the heating rods and the process temperature and by insulating the process vessel. Rod dT limits for these tests were constrained to 30 ºC during heat-up and 20 ºC during steady-state heating. The maximum dT that was observed during steady state heating was approximately 20 °C.

2.2 Test Protocol

2.2.1 Sample Description

There were two sample mixtures used for testing, a Tank 22 sample supernate composite and a Tank 22 sample slurry. Both sample mixtures were formed from a series of three Tank 22 slurry samples collected in 2016 and 2017 using three-liter samplers. Each of the original samples contained approximately 1 wt% insoluble solids. The first sample, HTF-22-16-118, contained approximately 1 liter, while the other two

samples, HTF-22-17-6 and HTF-22-17-34, each contained approximately 3 liters. Portions of the samples have been utilized previously for solids measurement. HTF-22-16-118 also previously received rudimentary chemical characterization.[21] Tank 22 sample slurry was exclusively a portion of sample HTF-22-17-6 slurry. This sample was previously determined to include 1.05 wt% insoluble solids. The Tank 22 sample supernate composite was a mixture of decanted supernate from the remaining portions of HTF-22-16-118, HTF-22-17-6, and HTF-22-17-34. Characterization of the Tank 22 supernate composite and slurry is contained in Appendix A.

The SC-18 SME product was used as an alternate source of glycolate for this testing to represent the minor components in the RCT during NGA processing that may impact the thermolytic HGR in Tank 22. SC-18 SME product was generated during Sludge Batch 9 NGA flowsheet qualification testing.[16] Adjusted SC-18 SME product supernate was prepared as follows:

- 44.121 g of supernate liquid was decanted from the settled solids of the SC-18 SME product.
- 1.664 g of sodium hydroxide solution was added to the supernate liquid to mimic the pH adjustment in the RCT. Sodium hydroxide (50 wt%) was added, targeting 0.5 M OH^- (assuming no buffering), and solids precipitated. Because buffering occurs, the final OH^- concentration in the mixture was less than 0.5 M. The 50 wt% sodium hydroxide used in this pH adjustment was from the same batch (from Univar USA Inc.) that was used for LTAD testing and that was shown to have a minimal TOC content (<4 mg/L).[20]
- After hydroxide adjustment, solids were removed by filtration through a 0.45-micron nylon filter.

2.2.2 Testing Parameters

The testing parameters were as follows.

- Measurement apparatus: nominally 1 L flow system, fluoropolymer vessel with fluoropolymer lid. Total volume (liquid and gas) of approximately 1.2 L.
- Test samples: see above
- Sample density: 1.025 g/mL at 26 °C
- Sample volume: approximately 1.0 L
- Sample mass: approximately 1030 g
- Equipment total gas volume: approximately 200 mL
- Target measurement purge rate: 3 mL/min at standard conditions (1 atm and 21.1 °C).
- Time to equilibrate vapor space for HGR measurement: It requires approximately 3.3 hours to achieve three vapor space volume turn-overs at standard conditions and 3 mL/min purge rate.
    - This condition is applicable for tests equilibrating below the boiling point temperature. Due to water vapor and increased gas temperature, this period is reduced for tests equilibrating at the boiling point temperature.
- Condenser cooling water set point: 10 °C
- Condenser gas output temperature: approximately 25 °C
- Heating rod temperature target: less than 20 °C above solution temperature when equilibrating at measurement temperature, less than 30 °C above solution temperature when heating to measurement temperature
- Mixer rate: nominally 100 to 300 rpm, or as needed for liquid mixing and foam control. This range is also applicable to the Tank 22 slurry sample test. Note that there is not visual confirmation of mixing.

2.2.3 Testing Process

The following tests were performed in sequence using separate aliquots of Tank 22 sample composite material.

Test 1: Tank 22 sample supernate with no glycolate added
Test 2: Tank 22 sample supernate with glycolate added as sodium glycolate
Test 3: Tank 22 sample supernate with glycolate added as adjusted SC-18 SME product supernate
Test 4: Tank 22 sample slurry with glycolate added as sodium glycolate

Tests 1 and 2 were performed the week of April 9, 2018 and Tests 3 and 4 were performed the week of April 16, 2018. The following are the detailed steps for performing each test.

Test 1. The testing process for Tank 22 sample supernate with no glycolate added was as follows.

- Load the system with approximately 1 L (1030 g) of the Tank 22 sample supernate material
- Agitate sample and initiate purge gas flow
- Heat to the near-ambient temperature of 30 °C
- Adjust purge gas flow to the measurement purge rate
- Allow the system to equilibrate and measure the HGR at the near-ambient temperature
- Increase purge and heat to the first elevated temperature of 60 °C
- Adjust purge gas flow to the measurement purge rate
- Allow the system to equilibrate and measure the HGR at the first elevated temperature
- Increase purge and heat to the second elevated temperature of 80 °C
- Adjust purge gas flow to the measurement purge rate
- Allow the system to equilibrate and measure the HGR at the second elevated temperature
- Increase purge and heat to the atmospheric pressure boiling point of the mixture, which is expected to be between 100 °C and 103 °C
- Adjust purge gas flow to the measurement purge rate
- Allow the system to equilibrate and measure the HGR at the third elevated temperature.
- Shutdown the system and unload the Tank 22 material
- Subsample the Tank 22 material for post-HGR chemical analysis
- Clean and reassemble the system

Test 2. The testing process for Tank 22 sample supernate with glycolate added as sodium glycolate was as follows.

- Load the system with approximately 1 L (1030 g) of the Tank 22 sample supernate material and 0.154 g of 99.1 wt% sodium glycolate (corresponding to 120 mg/L of glycolate)
- Agitate sample and initiate purge gas flow
- Heat to the near-ambient temperature of 30 °C
- Adjust purge gas flow to the measurement purge rate
- Allow the system to equilibrate and measure the HGR at the near-ambient temperature
- Increase purge and heat to the first elevated temperature of 60 °C
- Adjust purge gas flow to the measurement purge rate
- Allow the system to equilibrate and measure the HGR at the first elevated temperature
- Increase purge and heat to the second elevated temperature of 80 °C
- Adjust purge gas flow to the measurement purge rate
- Allow the system to equilibrate and measure the HGR at the second elevated temperature
- Increase purge and heat to the atmospheric pressure boiling point of the mixture, which is expected to be between 100 °C and 103 °C
- Adjust purge gas flow to the measurement purge rate
- Allow the system to equilibrate and measure the HGR at the third elevated temperature.

- Shutdown the system and unload the Tank 22 material
- Subsample the Tank 22 material for post-HGR chemical analysis
- Clean and reassemble the system

Test 3. The testing process for Tank 22 sample supernate with glycolate added as adjusted SC-18 SME product supernate was as follows.

- Load the system with approximately 1 L (1030 g) of the Tank 22 sample supernate material and 3.88 g of adjusted SC-18 SME product supernate corresponding to 120 mg/L of glycolate in the mixture. The actual amount of adjusted SC-18 SME product supernate added was 4.00 g, which is about 3% higher than the targeted amount.
- Agitate sample and initiate purge gas flow
- Heat to the near-ambient temperature of 30 °C
- Adjust purge gas flow to the measurement purge rate
- Allow the system to equilibrate and measure the HGR at the near-ambient temperature
- Increase purge and heat to the first elevated temperature of 60 °C
- Adjust purge gas flow to the measurement purge rate
- Allow the system to equilibrate and measure the HGR at the first elevated temperature
- Increase purge and heat to the second elevated temperature of 80 °C
- Adjust purge gas flow to the measurement purge rate
- Allow the system to equilibrate and measure the HGR at the second elevated temperature
- Increase purge and heat to the atmospheric pressure boiling point of the mixture, which is expected to be between 100 °C and 103 °C
- Adjust purge gas flow to the measurement purge rate
- Allow the system to equilibrate and measure the HGR at the third elevated temperature.
- Shutdown the system and unload the Tank 22 material
- Subsample the Tank 22 material for post-HGR chemical analysis
- Clean and reassemble the system

Test 4. The testing process for Tank 22 sample slurry with glycolate added as sodium glycolate was as follows.

- Load the system with approximately 1 L (1030 g) of the Tank 22 sample slurry material and 0.154 g of 99.1 wt% sodium glycolate (corresponding to 120 mg/L of glycolate)
- Agitate sample and initiate purge gas flow
- Heat to the near-ambient temperature of 30 °C
- Adjust purge gas flow to the measurement purge rate
- Allow the system to equilibrate and measure the HGR at the near-ambient temperature
- Increase purge and heat to the first elevated temperature of 60 °C
- Adjust purge gas flow to the measurement purge rate
- Allow the system to equilibrate and measure the HGR at the first elevated temperature
- Increase purge and heat to the second elevated temperature of 80 °C
- Adjust purge gas flow to the measurement purge rate
- Allow the system to equilibrate and measure the HGR at the second elevated temperature
- Increase purge and heat to the atmospheric pressure boiling point of the mixture, which is expected to be between 100 °C and 103 °C
- Adjust purge gas flow to the measurement purge rate
- Allow the system to equilibrate and measure the HGR at the third elevated temperature.
- Shutdown the system and unload the Tank 22 material
- Subsample the Tank 22 material for post-HGR chemical analysis

- Clean the system

Based on the thermocouple specification, temperature measurements should be attainable with a 2σ uncertainty of 2.2 °C. The addition of sodium glycolate reagent to Tank 22 supernate or slurry (Tests 2 and 4) to create a 120 mg/L glycolate solution should be attainable with a 2σ uncertainty of approximately 5 mg/L. Because of the analytical measurements involved with the addition of adjusted SME product, the creation of a 120 mg/L glycolate solution for Test 4 should be attainable with a 2σ uncertainty of approximately 24 mg/L.

2.3 Data Collection

2.3.1 Gas Handling and Analysis

Offgas from the tests was characterized using an Agilent series 3000 micro GC. Column-A collected data related to He, H_2, O_2, N_2, Kr, and CH_4, while column-B collected data related to CO_2 and N_2O. Due to limited GC sensitivity when using argon carrier gas (needed for hydrogen quantification), it was not possible to identify other oxides of nitrogen and carbon. The GC method was modified to quantify low quantities of hydrogen. The instruments have previously been used to quantify offgas from DWPF CPC demonstrations which generally have significantly higher gas generation rates. To quantify the low concentrations of hydrogen, sample injection times were increased by a factor of three relative to DWPF simulations. To improve sensitivity, the GC sensitivity mode was changed from normal to high. Because of these changes, the ability to accurately quantify oxygen and nitrogen has been sacrificed, although even with previous settings, the nitrogen results were of limited usefulness, due to low consistency. Raw chromatographic data were acquired by the GC from the offgas stream samples using a separate computer interfaced to the data acquisition computer (as described above). Sampling frequency was approximately one chromatogram every four minutes.

The GC was calibrated with a gas mixture containing nominally 50 ppmv hydrogen, 20.0 vol% oxygen, 0.5 vol% krypton, 1.0 vol% carbon dioxide, 0.5 vol% nitrous oxide, and the balance nitrogen. It was assumed that the GC response (peak area) was linear and proportional to the gas concentration. This assumption was demonstrated to be appropriate for hydrogen with several other hydrogen-bearing gas standards.[9] The calibrations were verified prior to and after completing a week of testing (before Test 1, after Test 2, before Test 3, and after Test 4). A 500 ppmv methane (balance air) gas standard was analyzed on the GC, to demonstrate methane detection effectiveness and to provide input data for estimating the methane LOQ.

Based on current and previous GC calibration data,[9] the limit of quantification (LOQ) for hydrogen was determined to be 2.3 ppmv, which corresponds to 5.6×10^{-8} ft^3 h^{-1} gal^{-1} at the sample volume and purge rate used in this testing. The limit of detection (LOD) was determined to be 1.2 ppmv, which corresponds to 2.8×10^{-8} ft^3 h^{-1} gal^{-1} at test conditions. Measurements below the LOQ are semi-quantitative and should only be applied in a qualitative manner, such as representing general trends (i.e., increasing or decreasing with time). Measurements above the LOD but below the LOQ should be interpreted as positive indications of the presence of hydrogen as distinguishable from the GC baseline measurement. However, measurement uncertainty and bias are greatly increased when below the LOQ, and thus measurement values below the LOQ should not be used in calculations and comparisons.

The primary purge gas contained 0.5 vol% krypton, 20.0 vol% oxygen, and 79.5 vol% nitrogen. Air purge was also available and used to partially flush the system between measurement conditions. The Kr-bearing purge gas (as compared to air) served several purposes. First, by using the measured krypton concentration, one could determine if the headspace of the reaction vessel had been purged of air. Second, unlike air, the purge had no helium and hydrogen, which could interfere with quantification of hydrogen produced from

radiolysis or thermolysis. Third, Kr measurements were used to adjust for bulk gas generation from the sample, air leakage into the system, and back-mixing at the GC.

The relationship identified in Equation 3 was used to calculate the HGRs. With this equation, it was assumed that flow out of the vessel was equal to flow into the vessel. The validity of this assumption was confirmed by checking that the measured Kr concentration was the same as the Kr concentration in the purge gas fed to the reaction vessel.

$$HGR = H2_{area} \times \frac{H2_{stdconc}}{H2_{stdarea}} \times \frac{Kr_{stdarea}}{Kr_{stdconc}} \times \frac{Kr_{purgegas}}{Kr_{area}} \times F_{in} \times \frac{\rho}{m} \times 8.020 \times 10^{-6}$$ Equation 3

where,

HGR = H_2 generation rate, $ft^3 \cdot h^{-1} \cdot gal^{-1}$

$H2_{area}$ = GC H_2 response for a gas sample

$H2_{stdconc}$ = Concentration of H_2 calibration gas, ppmv

$H2_{stdarea}$ = Average of five GC responses from the H_2 calibration gas

F_{in} = flow of Kr-bearing purge gas into the reaction vessel, sccm

ρ = density of sample, $g \cdot mL^{-1}$

m = mass of sample, g

8.020×10^{-6} = conversion factor, $ft^3 \cdot min \cdot mL \cdot cc^{-1} \cdot gal^{-1} \cdot ppmv^{-1} \cdot hr^{-1}$

$Kr_{purgegas}$ = Concentration of Kr in the purge gas, not including any supplemental air, vol%

Kr_{area} = GC Kr response for a gas sample

$Kr_{stdconc}$ = Concentration of Kr calibration gas, vol%

$Kr_{stdarea}$ = Average of five GC responses from the Kr calibration gas

The gas volume basis of the HGR measurements reported in this document is at a standard condition of 25 °C and 1 atm. to match the CSTF HGR calculation standard condition. Purge rates quoted in this document are at a standard condition of 21.1 °C and 1 atm. to match the standard condition of the HGR measurement apparatus.

The software package GUM workbench[22] was used to determine the partial derivatives used to calculated the overall uncertainty for the above equations. The overall uncertainty (using these derivatives) and one sigma uncertainties in the variables was then used to calculate uncertainties for all the data points using the software package JMP Pro Version 11.2.1.[23]

2.3.2 Analytical Methods for Sample Analysis

Table 2-1 lists the analyses for the HGR test feeds and products. Characterization methods include Inductively Coupled Plasma – Atomic Emissions Spectroscopy (ICP-AES); Inductively Coupled Plasma – Mass Spectroscopy (ICP-MS); Ion Chromatography for Anions (ICA); titration for total base, free hydroxide, and other base excluding carbonate; Total Inorganic Carbon/Total Organic Carbon (TIC/TOC); and Cold Vapor Atomic Absorption (CVAA) for mercury; Gas Chromatography Cold-Vapor Atomic Fluorescence Spectroscopy (GCCVAFS) for monomethyl mercury; Volatile Organics Analysis (VOA) for propanal and other volatile organic compounds; Semi-Volatile Organics Analysis (SVOA) for

hexamethyldisiloxane (HMDSO), trimehtylsilanol (TMS) and other semi-volatile organic compounds, and gamma scan.

Table 2-1. Analytical Plan for HGR testing feeds and products.

Tank 22 sample slurry	Tank 22 sample supernate composite	Adjusted SC-18 SME product supernate	Post-HGR supernate
• Density • Aqua Regia digestion o ICP-AES o ICP-MS o CVAA • Alkali fusion digestion o ICP-AES o Gamma scan	• Density • ICP-AES • ICP-MS • ICA • TIC/TOC • Titration • CVAA[a] • GCCVAFS • VOA • SVOA	• Density • ICP-AES • ICP-MS • ICA • TIC/TOC • Titration • CVAA[a] • GCCVAFS • VOA • SVOA	• Density • ICP-AES • ICA • TIC/TOC • Titration • CVAA[a]

[a]with permanganate digestion

2.4 Quality Assurance

Requirements for performing reviews of technical reports and the extent of review are established in manual E7 2.60.[24] SRNL documents the extent and type of review using the SRNL Technical Report Design Checklist contained in WSRC-IM-2002-00011, Rev. 2.[25] Data are recorded in the electronic laboratory notebook system as notebook/experiment numbers A6583-00142-19 and 20, and other associated notebooks/experiments.

3.0 Results and Discussion

3.1 Tank 22 Hydrogen Generation Rate Measurements

3.1.1 Measurement Test Profiles

Appendix B contains full measurement profiles from the HGR testing. Included are the process temperature (T, °C), the ratio of the Kr tracer measured concentration (Kr) to feed Kr concentration (Kr_0), the Kr-containing purge gas flow rate (sccm), the total purge gas flow rate (sccm), and the HGR ($ft^3\ h^{-1}\ gal^{-1}$). The LOQ of the HGR adjusted for Kr/Kr_0 is also indicated.

Analysis of the data assumes the equipment functions like a classic continuous stirred tank reactor. Hence, until sufficient purge gas has been supplied to provide ~3 full vapor space turnovers, the test is still in a transition period approaching a pseudo steady-state. Until $Kr/Kr_0 \geq 0.8$, the HGR is in transition (i.e., having achieved only 1-2 vapor space turnovers). Although hydrogen concentration measurements are valid during transition, the HGR values during transition are less reliable for projecting the pseudo steady-state HGR. During the early period of data collection, the purge rate is altered to allow for quantifying the degree of approach to steady-state conditions. Hence, values before $Kr/Kr_0 \approx 0.8$ are not useful in determining the pseudo steady-state HGR. The report only provides HGR values adjusted for measured tracer in the non-condensable offgas when $Kr/Kr_0 \geq 0.8$. The target of three vapor space turnovers corresponds to $Kr/Kr_0 \approx 0.99$. Requiring measured attainment of $Kr/Kr_0 \geq 0.99$ is impractical due to flow controller uncertainty, GC analysis uncertainty, uncondensed water vapor, and possible trace production of gasses such as N_2.

3.1.2 Steady HGR Measurement Results

Figure 3-1 through Figure 3-4 display HGR data for the Tank 22 tests. The data reported for each test is when $Kr/Kr_0 \geq 0.8$, which corresponds to between one and two vessel headspace turn-overs. The target is to reach at least three vessel headspace turnovers by the completion of the HGR measurement, which occurs after approximately 3.5 hours except at the boiling condition. Three vessel headspace turnovers occur more quickly at boiling because the water vapor in the vessel headspace contributes to volume. For all cases except two, HGR was evaluated based on the average of the final 15 gas measurements of the equilibration period (i.e., the final 60 minutes). For the two exceptions (Test 1 at boiling and Test 3 at 30 °C), HGR was evaluated based on the average over the final 8 gas measurements (i.e., the final 30 minutes) due to the calculated HGR only reaching a steady condition for that period (as defined in Section 2.2.2). Time zero on the figures corresponds to the time that the target temperature was attained. As seen in Appendix B, for each test, the measurements were performed in series from lowest to highest temperature on the same sample aliquot. The LOQ value is an approximate minimum value for the LOQ (calculated for $Kr/Kr_0 = 1$, which is applicable only near the end of each test condition). Although the LOQ for hydrogen concentration is constant, the LOQ for HGR decreases with testing time as Kr/Kr_0 increases toward one.

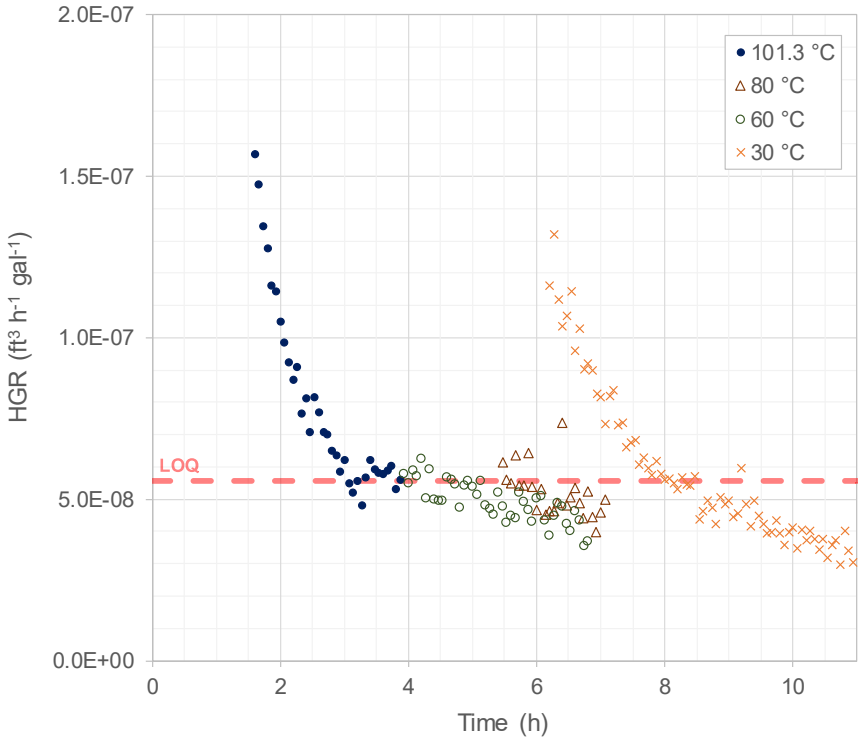

Figure 3-1. HGR measured during Test 1, Tank 22 sample supernate with no glycolate added.

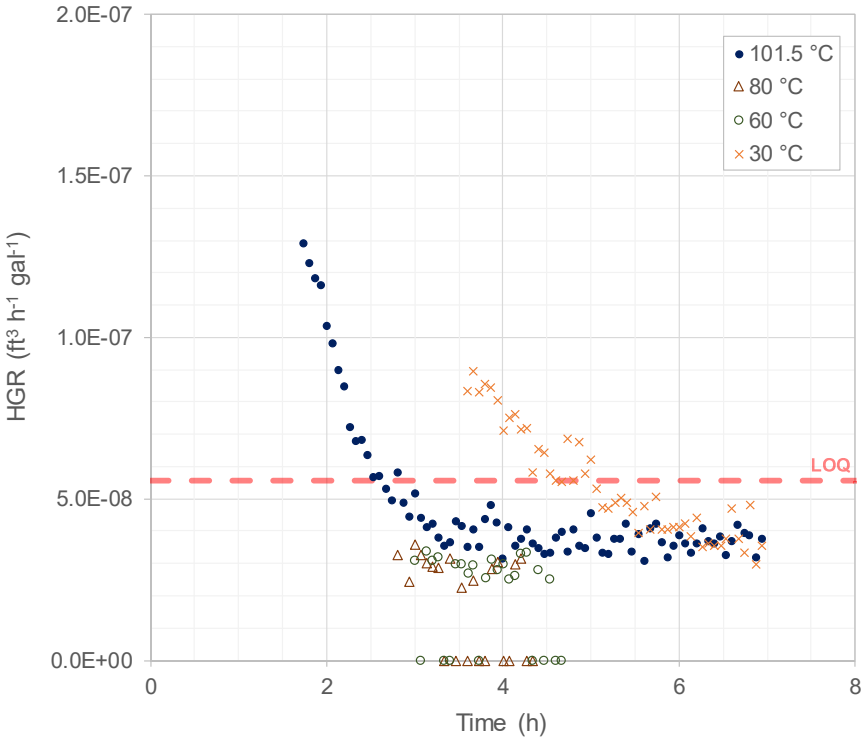

Figure 3-2. HGR measured during Test 2, Tank 22 sample supernate with 120 mg/L glycolate added as sodium glycolate.

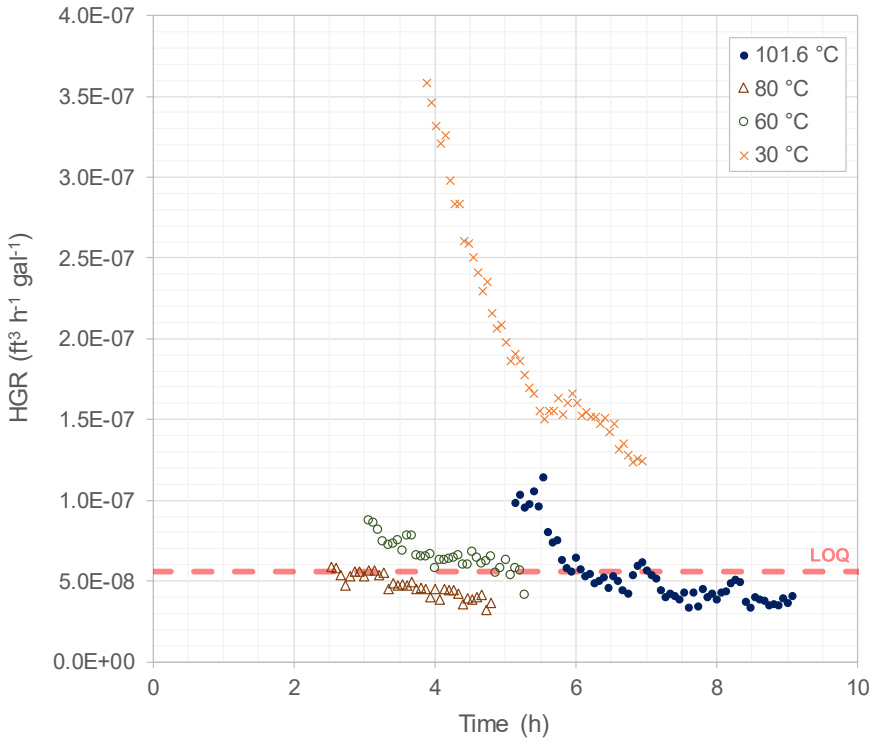

Figure 3-3. HGR measured during Test 3, Tank 22 sample supernate with 120 mg/L glycolate added as adjusted SC-18 SME product supernate.

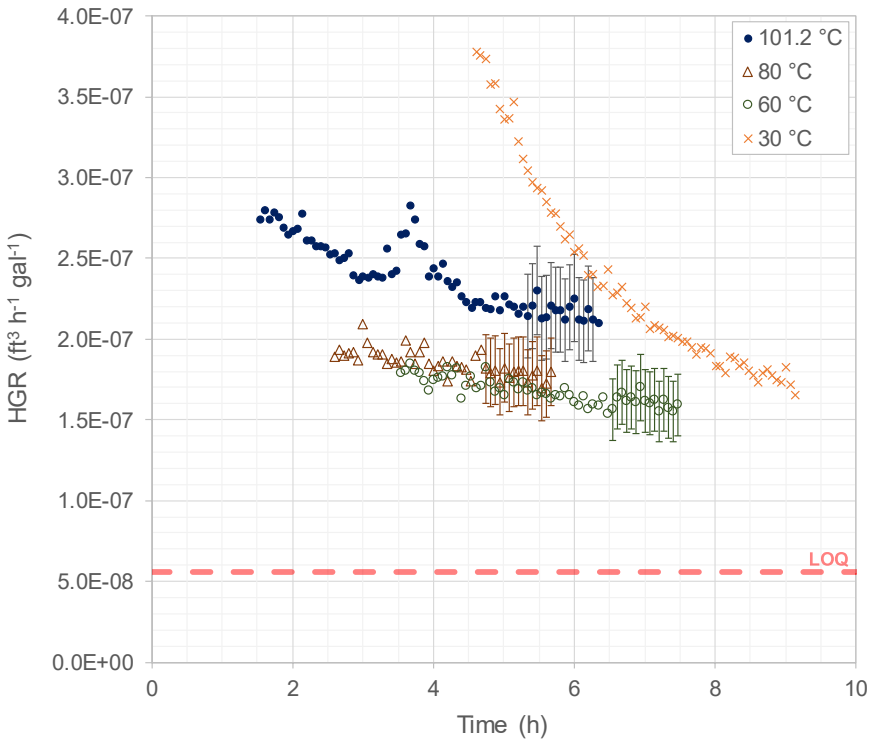

Figure 3-4. HGR measured during Test 4, Tank 22 sample slurry with 120 mg/L glycolate added as sodium glycolate.

Table 3-1 contains a compilation of the Tank 22 HGR measurements from the four tests. The table also indicates whether the sample supernate composite or the sample slurry was used, the amount of glycolate added, and whether the source of glycolate was reagent sodium glycolate or pH adjusted SME product from Shielded Cells NGA run SC-18. Measurements that were below the LOQ are listed in Table 3-1 as the LOQ is preceded by a less-than sign. In some cases, the HGR did not exceed the LOQ for all 10 or 15 data points. In those cases, values both above and below the LOQ were used in averages and the average measurement is preceded by "≤" in Table 3-1. Some of the results at near ambient conditions (30 °C) appeared to be transient hydrogen measurements that are not applicable toward determining a generation rate for hydrogen. These transient cases are discussed in Section 3.1.4.

Table 3-1. Results of Tank 22 HGR measurements.

Test	Sample	Glycolate		HGR (ft^3 h^{-1} gal^{-1})			
		Quantity	Source	30 °C	60 °C	80 °C	101.2 – 101.6 °C
1	supernate	0 mg/L	not applicable	< 5.6E-08	< 5.6E-08	< 5.6E-08	≤ 5.8E-08
2	supernate	120 mg/L	sodium glycolate	< 5.6E-08	< 5.6E-08	< 5.6E-08	< 5.6E-08
3	supernate	120 mg/L	SC-18 SME product	1.4E-07[a]	≤ 5.6E-08	< 5.6E-08	< 5.6E-08
4	slurry	120 mg/L	sodium glycolate	1.8E-07[a]	1.61E-07 ± 12%	1.78E-07 ± 12%	2.17E-07 ± 12%

[a] Measurements at 30 °C appear to be transient, decreasing HGR for which statistics were not applied.

In the three tests with the Tank 22 sample supernate composite (Tests 1 through 3), most results were below the LOQ of 5.6×10^{-8} ft^3 h^{-1} gal^{-1}. Only three conditions (i.e., Test 1 at boiling and Test 3 at 30 °C and 60 °C) averaged at or above the LOQ.

Figure 3-1 displays the HGR for Test 1, Tank 22 sample supernate without glycolate. HGR Test 1 is the control test applicable to the organics currently present in Tank 22 and without future implementation of the DWPF Nitric-Glycolic Acid flowsheet. Test 1 HGR measurements at 30, 60, and 80 °C were ultimately below the LOQ of 5.6×10^{-8} ft^3 h^{-1} gal^{-1}. The average HGR at the end of Test 1 at boiling was 5.8×10^{-8} ft^3 h^{-1} gal^{-1}, which is just above the LOQ and is an average of measurements both above and below the LOQ. As Test 1 had no added glycolate, the small HGR measured at boiling is possibly due to the thermolysis HGR from the organics presently in Tank 22. Alternatively, and supported by the Test 2 and 3 measurements, it is possible that the hydrogen generated at boiling in Tank 22 is transient and would be reduced to less than the LOQ with a slightly longer equilibration time. The measurement at 80 °C took longer than expected to reach the target Kr/Kr_0 because of flow irregularities in the condenser. After the condenser apparatus was adjusted, the offgas measurements stabilized and the HGR at the 80 °C condition was measured (below the LOQ).

Figure 3-2 displays the HGR for Test 2, Tank 22 sample supernate with 120 mg/L glycolate added as sodium glycolate. HGR Test 2 is applicable to both the organics currently present in Tank 22 plus the expected glycolate carryover from the future implementation of the DWPF Nitric-Glycolic Acid flowsheet. Test 2 HGR measurements were below LOQ for all temperatures. Figure 3-3 displays the HGR for Test 3, Tank 22 sample supernate with 120 mg/L glycolate added as adjusted SC-18 SME product. HGR Test 3 is applicable to both the organics currently present in Tank 22 plus the expected glycolate and other potential DWPF material carryover from the DWPF Nitric-Glycolic Acid flowsheet. Test 3 at 30 °C showed a non-steady decreasing HGR that was approximately 1.4×10^{-7} ft^3 h^{-1} gal^{-1} at the end of the measurement. The decreasing HGR carried over into the start of the measurement at 60 °C. The average HGR at the end of Test 3 at 60 °C was 5.6×10^{-8} ft^3 h^{-1} gal^{-1}, which is right at the LOQ and is also an average of measurements both above and below the LOQ. Test 3 HGR measurements at 80 °C and boiling were below LOQ. The Test 3 measurement at boiling took longer than expected to reach the target Kr/Kr_0 because of flow irregularities in the condenser. After the condenser apparatus was adjusted, the offgas measurements stabilized and the HGR at the boiling condition was measured (below the LOQ). Because the HGR at elevated temperatures for Tests 2 and 3 were below the LOQ and seemingly lower than the control test HGR (Test 1 at boiling), there is no apparent HGR in Tank 22 ($<5.6\times10^{-8}$ ft^3 h^{-1} gal^{-1}) that would be attributable to thermolysis caused by the DWPF Nitric-Glycolic Acid flowsheet. By extension, based on Tests 2 and 3, there is also no apparent HGR in Tank 22 ($<5.6\times10^{-8}$ ft^3 h^{-1} gal^{-1}) that would be attributable to thermolysis of the current tank organics.

Figure 3-4 displays the HGR for Test 4, Tank 22 sample slurry with 120 mg/L glycolate added as sodium glycolate. In Test 4, the HGR measurement results at all temperatures were above the LOQ. Because of the inclusion of sludge in Test 4, there was increased HGR from radiolysis observed. The Test 4 HGR measurement at 30 °C was 1.77×10^{-7} ft^3 h^{-1} gal^{-1}. The HGR result of 1.61×10^{-7} ft^3 h^{-1} gal^{-1} at 60 °C showed a slight decrease from the 30 °C condition. The HGR measurements at 80 and 101.2 °C were 1.78×10^{-7} ft^3 h^{-1} gal^{-1} and 2.17×10^{-7} ft^3 h^{-1} gal^{-1}, respectively. The error bars seen in Figure 3-4 represent the 95% confidence interval (CI) on individual HGR measurements and indicate the points used to calculate the average HGR measurement for the elevated temperature conditions. The HGR results at each temperature showed decreasing trends with measurement time. Thus, the Test 4 HGR results may contain additional bias not represented by the reported CI.

From the Test 4 results, there is not a strong temperature dependence of the HGR over the range of temperatures. It is difficult to accurately quantify the differences between the HGR measurements at the different temperatures due to the measurement uncertainty and the downward trends with measurement

time. Using only the HGR measurement data at 60, 80, and 101.2 °C, the approximate apparent activation energy for the overall hydrogen generation is 7.5 kJ/mol, which is very low compared to typical temperature-dependent reactions (such as the 89.6 and 113 kJ/mol in the models of Equations 1 and 2, respectively). The low apparent activation energy indicates that the radiolytic component of HGR in Test 4 is dominant and is masking the possible presence of a small thermolytic HGR. The magnitude of potential increase in HGR with increasing temperature for Test 4 is small and is on the order of the results (at or below LOQ) for Tests 1 through 3. Thus, it is indeterminate from this testing Tank 22 whether the presence of sludge solids impact the thermolytic HGR.

Through uncertainty analysis, the 95% CI for Test 4 HGR measurement results are ±12%. Due to the Test 1 and 3 results preceded by "≤" being influenced by the proximity to the LOQ, the 95% CI for those results are estimated as ±25%. The uncertainty is not reported for the LOQ values and for the 30 °C measurements that appeared to be transient and decreasing. For all cases, the uncertainty analysis does not include factors of the testing that may bias the results, such as consumption of organic reactants, incubation periods, non-steady generation of hydrogen, and slow release of dissolved hydrogen.

3.1.3 Comparison to Thermolytic Hydrogen Generation Rate Predictions

As explained in Section 1.2, thermolytic HGR in radioactive waste can be evaluated using two methods (i.e., expression derived by Hu and Ashby, respectively)[2,10] derived from Hanford Tank Farm data and related experimentation.

The Hu expression (Equation 1) relates thermolytic HGR in Hanford tanks with an Arrhenius expression that is first order in TOC concentration and 0.4 order in aluminum concentration. An empirically determined reactivity factor term is included in the fit. Values of 0.6 are used for newer-style Hanford tanks while 0.3 is used for older-style Hanford tanks.

The Ashby simulant work was specific for glycolate under a relatively narrow concentration range. Crawford and King extended the work for extrapolation to lower aluminum concentrations and to temperatures below 90 °C. Their relationship based on Ashby's work (Equation 2) is first order in TOC, aluminum, and nitrite concentrations and inverse first order in hydroxide concentration. The Ashby relationship typically predicts lower thermolytic HGR than the Hu equation for SRS wastes. The concentrations in Ashby's experimental work were significantly greater than the relatively dilute Tank 22 material (e.g., Na concentration is 8.79 M in Ashby salt simulant SY1-SIM-91B-NG and 0.592 M in Tank 22 sample supernate composite; Al concentration is 1.54 M in Ashby simulant and 0.000518 M in Tank 22).

Table 3-2 contains predictions for thermolytic HGR for Tank 22 sample material. The inputs for the HGR predictions are the TOC and glycolate based solely on the 120 mg/L of added glycolate and the measured values for aluminum (5.18×10^{-4} M), nitrite (2.47×10^{-1} M), and hydroxide (1.89×10^{-1} M) in the supernate sample composite (analyzed prior to heating in an HGR test). The predictions did not consider the non-glycolate TOC contained in the Tank 22 material or the increase in aluminum concentration encountered in the Test 4 HGR measurement that used Tank 22 slurry. For the Hu expression, a reactivity factor of 1 was used. Even at boiling temperature, thermolytic HGR calculated from the Hu expression (4.8×10^{-8} $ft^3\ h^{-1}\ gal^{-1}$) is less than the LOQ of 5.6×10^{-8} $ft^3\ h^{-1}\ gal^{-1}$ for the HGR flow system. Predictions from expression based on the Ashby work are even lower, 2.1×10^{-10} $ft^3\ h^{-1}\ gal^{-1}$ at the boiling condition. Based on the boiling condition where the Hu expression gives the highest value, the measured value for Tank 22 supernate that was below the LOQ indicates that HGR was not significantly higher than expected from thermolysis in Tank 22 with added glycolate.

Table 3-2. Tank 22 thermolytic HGR from 120 mg/L glycolate with predictions from the Hu and Ashby methods.

Tank 22 T (°C)	HGR Test 2 ($ft^3\ h^{-1}\ gal^{-1}$)	Hu HGR (r_f=1) ($ft^3\ h^{-1}\ gal^{-1}$)	Ashby HGR ($ft^3\ h^{-1}\ gal^{-1}$)
101.6	< 5.6E-08	4.8E-08	2.1E-10
80	< 5.6E-08	8.2E-09	2.3E-11
60	< 5.6E-08	1.3E-09	2.3E-12
30	< 5.6E-08	5.4E-11	4.0E-14

The purpose of HGR measurements with Tank 22 radioactive waste material was to ensure that HGR was not higher than expected. Given the LOQ, it is indeterminant whether Tank 22 HGR is higher than expected from the Hu or Ashby equations. This is an important observation because the dilute concentrations of most components in Tank 22 are significantly outside the range of where these models were developed. Both Hu and Ashby models focused on more concentrated solutions (multi-molar hydroxide and salt concentrations) where hydrogen generation is more prevalent. Further simulant testing is underway to develop an HGR model that is applicable to a wide range of SRS CSTF conditions, including more dilute waste such as Tank 22.

3.1.4 Transient Hydrogen Release

As mentioned previously, HGR measurements are not applicable for transition periods between measurement conditions, but hydrogen concentration measurements remain accurate during those periods. There were two common times during transition and equilibration where transient peaks of hydrogen were noted: 1) the period between establishment of mixing and purge and the equilibration of the near-ambient temperature 30 °C measurement condition; and 2) the period as the material is heated to boiling through the initial boiling period.

Figure 3-5 contains hydrogen concentration measurements from the start of each HGR measurement test through the completion of equilibration at the 30 °C measurement condition. The 30 °C temperature is attained at 13 to 19 minutes after the start of the test. Three of the tests showed peaks in hydrogen concentration of approximately 25 ppmv just after 2 hours after the start of data collection while the other test had a peak hydrogen concentration of approximately 5 ppmv. After this initial peak of hydrogen is released, similar such peaks are not released at 60 and 80 °C elevated temperatures.

These initial peaks are hypothesized to be due to the release of hydrogen from the liquid phase upon the establishment of mixing and purge (i.e., dissolved hydrogen). Hydrogen that is produced slowly by radiolysis during the sample storage period prior to HGR testing can build up in the liquid phase due to being stored in closed bottles. Even though hydrogen diffusion through the plastic bottles would be significant on the time scale of sample storage, some buildup in the liquid is expected. When purge air contacts the agitated mixtures, the liquid phase hydrogen is slowly released. This mechanism for an initial release of dissolved hydrogen is relatively prominent in the Tank 22 test because hydrogen solubility is expected to be higher in Tank 22 than in most CSTF tanks because Tank 22 material is relatively dilute. The initial peak is so broad that it impacted the 30 °C measurement for several of the tests and contributed to potentially unnecessary delay in testing.

The reason that Test 2 had initial peak concentrations of hydrogen much lower than the other three tests is that the period of high total purge rate used during heating to 30 °C was established earlier in the sample loading process and thus was performed for a longer period for Test 2 than for the other tests. This longer period of high purge removed liquid phase hydrogen more quickly and resulted in overall lower initial peak of hydrogen concentration. This observation also supports the hypothesized mechanism. It is recommended that this extended period of higher initial purge rate be performed in future to limit interference of radiolytic hydrogen remaining in the sample liquid phase on the subsequent HGR measurement.

Figure 3-6 contains a plot of the hydrogen concentration measurement from the initiation of heating from 80 °C to boiling through the completion of equilibration at the boiling measurement condition. The boiling measurement condition was attained 43 to 64 minutes after adjusting the temperature set point (time zero on the plot). These peaks in hydrogen concentration at 5 to 10 ppmv of hydrogen would correspond to very short-term hydrogen generation and/or release from the liquid phase being diluted into the vessel vapor space with a low purge flow. These hydrogen peaks are likely due to solubility changes and steam stripping that further removes hydrogen from the liquid phase or small bubbles near or at boiling. Testing with the HGR flow system is designed to measure steady generation rates and is not capable of quantifying very short-term hydrogen generation or release rates. Test 4 is the only case where the equilibrated hydrogen concentration (~8 ppmv) is near the peak at boiling.

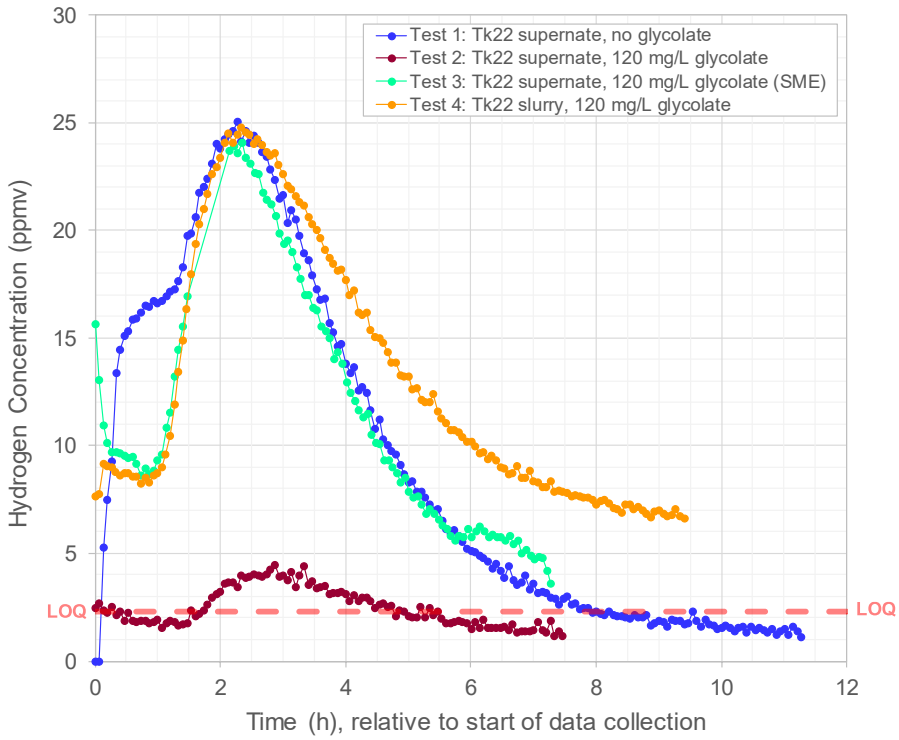

Figure 3-5. Hydrogen measured after loading sample, establishing purge, and heating to the near-ambient condition of 30 °C.

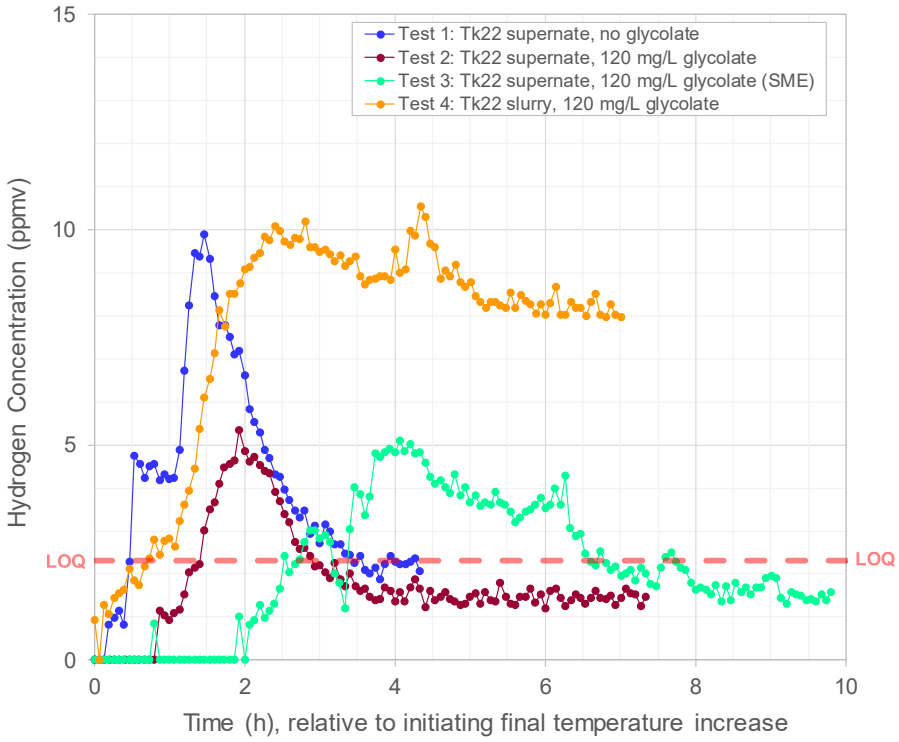

Figure 3-6. Hydrogen measured during transition to and at boiling condition.

3.2 Other Gas Generation

The GC can detect methane, carbon dioxide, and nitrous oxide. For these runs, the GC was calibrated for these gases using relatively high concentrations – 500 ppmv methane, 1% carbon dioxide, and 0.5% nitrous oxide. None were detected.

Since the Tank 22 experiments, SRNL has evaluated the GC with a 2 ppmv and 10 ppmv methane standard (balance air in both cases). The GC was unable to detect 2 ppmv methane. The 10 ppmv methane gas could be detected and quantified. Ten runs of this calibration gas yielded a relative standard deviation of 15%. Based on the 10 ppm methane calibration gas, the GC's LOD is less than 10 ppmv. Using an Environmental Protection Agency (EPA)[26] and Taylor[27] based methodology, the methane LOQ is approximately 14 ppmv.

3.3 Tank 22 Sample Analysis

Appendix A contains the full set of analytical results for the samples from this work. Analyses of test feed materials included the Tank 22 slurry sample, the Tank 22 supernate composite, the adjusted SC-18 SME product. Analyses also included the supernates associated with the material after the conclusion of each HGR test (henceforth referred to as "post-HGR").

A summary of key supernate data is contained in Table 3-3. There is no evidence of glycolate decomposition during the HGR measurements. Glycolate was added in Tests 2, 3, and 4 at levels of 1.33×10^{-3} M (120 mg/L), and the resulting post-HGR solution analysis showed 1.75×10^{-3}, 2.33×10^{-3}, and 1.89×10^{-3} M, respectively. All the applicable post-HGR analyses for glycolate were greater than the concentrations corresponding to the amounts of glycolate added. Much of this discrepancy is likely due to analytical uncertainty. Additionally, Test 3 relied on an initial analysis of the adjusted SME product and

had an approximately 3% larger amount fed than targeted. Uncertainty in the initial adjusted SME product analysis may have contributed to a larger addition of glycolate to Test 3 than targeted.

Table 3-3. Select analytical results from the supernate composite (pre-HGR) and the post-HGR supernates.

analyte	method	units	1σ (%)	Supernate Composite[a]			Post Test 1			Post Test 2			Post Test 3			Post Test 4		
				average	RSD	*n*	average	RSD	*n*	average	RSD	*n*	average	RSD	*n*	average	RSD	*n*
density	gravimetric	g/mL		1.025	0.3%	2	1.026	0.1%	2	1.028	0.1%	2	1.029	0.1%	2	1.034	1.3%	5
Na^+	ICP-ES	M	10	5.92E-01	0.6%	4	5.81E-01	2.6%	2	5.94E-01	2.6%	2	6.22E-01	4.3%	3	5.81E-01	1.1%	3
OH^-	titration	M	10	1.89E-01	3.9%	4	1.71E-01	2.5%	2	1.89E-01	1.1%	3	1.84E-01	--	1	1.92E-01	--	1
NO_2^-	IC	M	10	2.47E-01	10%	4	2.59E-01	1.2%	2	2.52E-01	3.7%	2	2.49E-01	0.5%	3	2.53E-01	1.8%	2
NO_3^-	IC	M	10	6.45E-02	1.1%	4	5.87E-02	12.0%	2	7.64E-02	13.0%	2	7.01E-02	0.1%	3	7.68E-02	1.3%	2
$Al(OH)_4^-$	ICP-ES	M	10	5.18E-04	4.5%	4	4.32E-04	3.0%	2	4.35E-04	0.6%	2	4.58E-04	2.8%	3	2.44E-03	0.6%	3
CO_3^{2-}	TIC/TOC	M	10	4.71E-02	1.2%	4	4.23E-02	2.2%	2	4.22E-02	0.5%	3	4.27E-02	--	1	4.10E-02	--	1
SO_4^{2-}	IC	M	10	6.30E-03	3.2%	4	6.22E-03	5.1%	2	6.81E-03	3.3%	2	6.48E-03	0.5%	3	5.74E-03	1.4%	2
CHO_2^-	IC	M	10	*<2.2E-03*	--	4	*<2.2E-03*	--	2	*<2.2E-03*	--	2	2.41E-03	0.5%	3	*<2.2E-03*	--	2
$C_2O_4^{2-}$	IC	M	10	2.56E-03	1.0%	4	2.22E-03	1.1%	2	2.29E-03	1.8%	2	2.78E-03	0.5%	3	2.31E-03	0.7%	2
$C_2H_3O_3^-$	IC	M	10	*<1.3E-04*	--	4	*<1.3E-04*	--	2	1.75E-03	1.6%	2	2.33E-03	2.0%	3	1.89E-03	1.5%	2
F^-	IC	M	10	*<5.3E-03*	--	4	*<5.3E-03*	--	2	*<5.3E-03*	--	2	1.86E-03	0.4%	3	*<5.3E-03*	--	2
Cl^-	IC	M	10	*<2.8E-03*	--	4	*<2.8E-03*	--	2	*<2.8E-03*	--	2	4.71E-04	0.6%	3	*<2.8E-03*	--	2
TOC	TIC/TOC	mg C/L	10	1.03E+02	0.9%	4	*<2.0E+01*	--	2	4.28E+01	6.1%	3	6.16E+01	--	1	3.91E+01	--	1
TMS	SVOA	mg/L	20	2.20E+01	--	1	--	--	0	--	--	0	--	--	0	--	--	0
CH_3Hg^+	GCCVAFS	mg/L	20	2.29E+00	--	1	2.40E+00	--	1	--	--	0	--	--	0	2.55E+00	--	1
B	ICP-ES	mg/L	10	4.85E+01	1.5%	4	4.17E+01	2.0%	2	4.10E+01	0.0%	2	4.45E+01	0.8%	3	4.07E+01	0.8%	3
Fe	ICP-ES	mg/L	11	2.22E+00	32%	4	*<4.1E-01*	--	2	*<4.1E-01*	--	2	4.74E-01	2.2%	3	*<4.1E-01*	--	3
Hg	CVAA	mg/L	20	1.71E+02	1.4%	4	2.25E+02	--	1	2.17E+02	--	1	2.21E+02	--	1	3.65E+02	--	1
K	ICP-ES	mg/L	15	2.97E+01	24%	4	3.24E+01	3.1%	2	2.51E+01	2.3%	2	2.80E+01	6.9%	3	2.86E+01	--	1
Li	ICP-ES	mg/L	10	4.99E+01	1.3%	4	4.79E+01	1.3%	2	4.73E+01	0.3%	2	5.02E+01	0.6%	3	4.34E+01	0.9%	3
P	ICP-ES	mg/L	20	*<1.0E+01*	--	4	5.74E+00	2.7%	2	5.25E+00	1.8%	2	5.57E+00	3.4%	3	*<1.8E+01*	--	3
Si	ICP-ES	mg/L	10	2.65E+02	1.0%	4	2.34E+02	1.2%	2	2.34E+02	0.3%	2	2.40E+02	0.6%	3	1.97E+02	0.3%	3

[a]The supernate composite is the supernate material prior to initiating tests and thus does not contain glycolate.

Comparing the supernate composite to the post-HGR supernates, most of the major salt components appeared to stay constant through the testing within analytical uncertainty. Additional aluminum appears to have gone into solution during Test 4, which included sludge solids and was heated to boiling. Mercury concentration was measured as 171 mg/L in the supernate feed composite, approximately 220 mg/L in the post-HGR samples from Tests 1, 2, and 3, and 365 mg/L in the post-HGR sample from Test 4. A portion of the originally insoluble mercury in the Tank 22 slurry apparently became soluble during Test 4. It is uncertain whether this is due to the heating of the slurry to boiling, the addition of 120 mg/L glycolate, or both factors. Because phase separation was by decanting rather than filtering, suspended insoluble or immiscible mercury may also be present. In the subset of these samples where its measurement was performed, methylmercury averaged approximately 2.4 mg/L, which is approximately 1% of the total mercury. Methylmercury may be biased low due to sample handling, as previous Tank 22 analysis for methylmercury showed 31.2 mg/L with a 7.4% relative standard deviation.[28]

TMS was measured in the supernate composite as 22 mg/L. No other SVOA or VOA species (including propanal) were identified with a detection limit of 1 mg/L. TMS introduces a potential for formation of methane during HGR testing, though none was noted. No additional organic compounds were identified that would be expected to lead to hydrogen or other flammable gas formation.

4.0 Conclusions

The majority of the test conditions for the Tank 22 supernate HGR measurements gave results below the LOQ for HGR of 5.6×10^{-8} ft^3 h^{-1} gal^{-1}. The introduction of glycolate into Tank 22 supernate at 120 mg/L both from reagent sodium glycolate and from adjusted SME product did not increase the HGR at boiling temperatures. Testing with Tank 22 slurry resulted in measurable HGR at all temperatures that ranged from of 1.61×10^{-7} ft^3 h^{-1} gal^{-1} to 2.17×10^{-7} ft^3 h^{-1} gal^{-1}. The majority of the measured HGR for the Tank 22 slurry is consistent with radiolytic hydrogen generation due to the presence of sludge solids and showed a weak relationship to temperature.

5.0 Recommendations

It is recommended to continue with the TTR and TTQAP testing of glycolic contribution to HGR with other waste matrices and conditions representing the balance of CSTF operations. Such data will aid in validation of models for HGR from the ongoing research and analysis.

The testing provides three recommendations for improvements in the SRNL experimental protocol.

- For future HGR testing with low purge rates, an improvement can be made at the start of the test if the purge is initiated at the elevated purge rate for an extended period with mixing and prior to heating. This will reduce the time necessary to flush the system of excess radiolytic hydrogen that built up in the sample during storage. The initial release of hydrogen causes a long period of transient hydrogen measurement that is not reflective of the actual HGR at ambient and other low temperatures.

- With limited sample volume, testing with actual waste at multiple temperatures is performed using the same sample aliquot. For this testing, measurements were performed in series starting with lowest temperature. This would be conservative for the lowest temperature measurements if there are small quantities of high hydrogen producing compounds that could get depleted quickly. However, in this testing, the lowest temperature measurements appear overly conservative due to the slow release of soluble hydrogen from the sample material. Where HGR testing of the same sample at multiple temperatures is involved, performing the HGR measurement at a higher temperature, such as the atmospheric pressure boiling temperature, first should be considered. Heating the mixture to boiling before ambient temperature and other elevated temperature HGR measurements would be an effective way to purge the system of radiolytic hydrogen that has built up during storage and is influencing lower temperature HGR measurements.

- Sample analysis needs should be evaluated when planning future actual-waste HGR testing. The evaluation should consider whether analysis of both pre-test and post-test sample material after the addition of sodium glycolate is necessary. The evaluation should also consider if improvements could be made to glycolate analysis in CSTF sample matrices for glycolate concentrations of 120 mg/L and below.

6.0 Acknowledgements

The authors would like to acknowledge the tremendous support of the shielded cells technicians, shielded cells management, analytical development personnel, machine shop personnel and glass shop personnel for assistance in carrying out this project. Tommy Edwards assisted with statistical analyses. SRNL management and SRR engineers and management contributed to oversight and experimental planning.

7.0 References

[1] Adu-Wusu, K., "Literature Review on Impact of Glycolate on the 2H Evaporator and the Effluent Treatment Facility (ETF)", SRNL-STI-2012-00132, Revision 0, May 2012.

[2] Ashby, E. C.; Annis, A.; Barefield, E. K.; Boatright, D.; Doctorovich, F.; Liotta, C. L.; Neumann, H. M.; Konda, A.; Yao, C. F.; Zhang, K.; and McDuffie, N. G., "Synthetic Waste Chemical Mechanism Studies", WHC-EP-0823, Revision 0, October 1994.

[3] Bryan, S. A.; Pederson, L. R.; and King, C. M., "Thermal and Radiolytic Gas Generation in Hanford High-level Waste", WM'00 Conference, February 27 - March 2, 2000.

[4] Crawford, C. L. and King, W. D., "Impacts of Glycolate and Formate Radiolysis and Thermolysis on Hydrogen Generation Rate Calculations for the Savannah River Site Tank Farm", SRNL-STI-2017-00303, Revision 0, August 2017.

[5] Condon, W. A., "Potentially inadequate recognition of the effect of organics on hydrogen generation rates in CSTF.", PI-2017-0003, February 28, 2017.

[6] Martino, C. J. and Edwards, T. B., "Run Plan for Tank 22 Sample Thermolysis Tests", SRNL-L3300-2018-00001, Revision 0, March 28, 2018.

[7] Clark, M. C., "Simulant and Radioactive Testing - Impact of Glycolate on Tank Farm", X-TTR-S-00067, Revision 2, July 9, 2018.

[8] Martino, C. J.; Woodham, W. H.; McCabe, D. J.; and Nash, C. A., "Task Technical and Quality Assurance Plan for Simulant and Radioactive Testing of the Impacts of Glycolate on Hydrogen Generation in the Savannah River Site Liquid Waste System", SRNL-RP-2017-00684, Revision 1, August 14, 2018.

[9] Martino, C. J.; Newell, J. D.; Woodham, W. H.; Pareizs, J. M.; Edwards, T. B.; Lambert, D. P.; and Howe, A. M., "Investigation of Thermolytic Hydrogen Generation Rate of Tank Farm Simulated and Actual Waste", SRNL-STI-2017-00611, Revision 0, November 2017.

[10] Hu, T. A., "Empirical Rate Equation Model and Rate Calculations of Hydrogen Generation for Hanford Tank Waste", HNF-3851, Revision 1, September 2004.

[11] Walker, D. D., "Organic Compounds in Savannah River Site High-Level Waste", WSRC-TR-2002-00391, Revision 0, September 30, 2002.

[12] Woodham, W. H., "Run Plan for Testing to Evaluate Importance of Major Salt Species on Thermolytic Production of Hydrogen from Glycolate", SRNL-L3300-2018-00011, Revision 1, September 26, 2018.

[13] Hay, M. S. and Martino, C. J., "Analysis of Condensate Samples in Support of the Antifoam Degradation Study", SRNL-STI-2015-00698, Rev. 1, February 2016.

[14] Bannochie, C. J.; Adamson, D. J.; and King, W. D., "Characterization of DWPF Recycle Condensate Tank Materials", SRNL-STI-2014-00603, Revision 1, April 2015.

[15] Kmiec, V. M. and Jabour, J. D., "Waste Laboratory Services – Laboratory Information Management System (WLS-LIMS) Data Generated to Scope Hydrogen Generation Rate (HGR) Experiments", X-ESR-S-00365, Revision 0, March 27, 2018.

[16] Newell, J. D.; Pareizs, J. M.; Martino, C. J.; Reboul, S. H.; Coleman, C. J.; Edwards, T. B.; and Johnson, F. C., "Actual Waste Demonstration of the Nitric-Glycolic Flowsheet for Sludge Batch 9 Qualification", SRNL-STI-2016-00327, Revision 1, March 9, 2017.

[17] Pareizs, J. M.; Newell, J. D.; Martino, C. J.; Crawford, C. L.; and Johnson, F. C., "Sludge Washing and Demonstration of the DWPF Nitric/Formic Flowsheet in the SRNL Shielded Cells for Sludge Batch 9 Qualification", SRNL-STI-2016-00355, Revision 0, October 2016.

[18] Stone, M. E.; Adamson, D. J.; Pak, D. J.; and Pareizs, J. M., "Hydrogen Generation Rate Measurement Apparatus: Final Design Package", SRNL-RP-2014-00866, Revision 0, September 2014.

[19] Stone, M. E.; Newell, J. D.; Smith, T. E.; and Pareizs, J. M., "WTP Waste Feed Qualification: Hydrogen Generation Rate Measurement Apparatus Testing Report", SRNL-STI-2016-00247, Revision 0, June 2016.

[20] Reboul, S. H.; Newell, J. D.; Pareizs, J. M.; and Coleman, C. J., "Low Temperature Aluminum Dissolution (LTAD) Real Waste Testing of the November 2017 Tank 51 Slurry Sample", SRNL-STI-2018-00179, Revision 0, June 2018.

[21] Pareizs, J. M., "Analytical Results for SRS Tank 22 Sample HTF-22-16-118 for Corrosion Control", SRNL-L3100-2017-00015, Revision 0, February 16, 2017.

[22] Metrodata GmbH, "GUM Workbench: User Manual for Version 1.3, 2.3, and 2.4", 2009.

[23] "SAS Institute Inc., JMP™ Pro, Ver. 11.2.1", Cary, NC, 2014.

[24] "Technical Reviews", Manual E7, Procedure 2.60, Revision 17, August 25, 2016.

[25] "Savannah River National Laboratory Technical Report Design Check Guidelines", WSRC-IM-2002-00011, Revision 2, August 2004.

[26] "Definition and Procedure for the Determination of the Method Detection Limit-Revision 2", 40 CFR, Part 136, Appendix B, 2017.

[27] Taylor, J. K., *Quality Assurance of Chemical Measurements*. Lewis Publishers, Inc.: Chelsea, MI, 1987.

[28] Bannochie, C. J., "Results of Preliminary Hg Speciation Testing on Tank 22 and Waste Concentrate Hold Tank (WCHT) Material", SRNL-L3100-2015-00079, Rev. 1, May 4, 2015.

Appendix A. Sample Characterization Tables

Table A-1. Analytical Results of Digested Tank 22 Slurry (HTF-22-17-6).

analyte	method	units	1σ (%)	Aqua regia			Peroxide fusion			Overall		
				average	RSD	*n*	average	RSD	*n*	best	RSD	*n*
Al	ICP-ES	mg/kg	10	5.11E+02	34%	3	1.22E+03	10%	3	1.22E+03	10%	3
B	ICP-ES	mg/kg	10	3.86E+01	3.3%	3	*<5.6E+01*	--	3	3.86E+01	3.3%	3
Ba	ICP-ES	mg/kg	10	6.04E+00	35%	3	*<1.5E+01*	--	3	6.04E+00	35%	3
Ca	ICP-ES	mg/kg	10	1.37E+02	35%	3	6.85E+02	8.3%	3	6.85E+02	8.3%	3
Cd	ICP-ES	mg/kg	14	5.91E+00	35%	3	*<2.7E+01*	--	3	5.91E+00	35%	3
Ce	ICP-ES	mg/kg	14	1.70E+01	--	1	*<7.5E+01*	--	3	1.70E+01	--	1
Cr	ICP-ES	mg/kg	15	1.62E+01	37%	3	3.69E+01	11%	3	3.69E+01	11%	3
Cu	ICP-ES	mg/kg	10	9.59E+00	15%	3	*<9.7E+01*	--	3	9.59E+00	15%	3
Fe	ICP-ES	mg/kg	10	1.50E+03	34%	3	2.49E+03	3.0%	3	2.49E+03	3.0%	3
Gd	ICP-ES	mg/kg	14	4.04E+00	41%	3	*<2.1E+01*	--	3	4.04E+00	41%	3
Hg	CVAA	mg/kg	20	1.23E+03	26%	3	--	--	--	1.23E+03	26%	3
La	ICP-ES	mg/kg	11	3.42E+00	34%	3	*<2.2E+01*	--	3	3.42E+00	34%	3
Li	ICP-ES	mg/kg	10	5.91E+01	7.1%	3	*<1.2E+02*	--	3	5.91E+01	7.1%	3
Mg	ICP-ES	mg/kg	10	6.51E+01	35%	3	9.24E+01	6.2%	3	9.24E+01	6.2%	3
Mn	ICP-ES	mg/kg	10	3.43E+02	34%	3	5.56E+02	3.2%	3	5.56E+02	3.2%	3
Na	ICP-ES	mg/kg	10	1.28E+04	7.2%	3	--	--	--	1.28E+04	7.2%	3
Ni	ICP-ES	mg/kg	10	1.17E+02	34%	3	*<1.9E+02*	--	3	1.17E+02	34%	3
S	ICP-ES	mg/kg	25	1.92E+02	6.5%	3	--	--	--	1.92E+02	6.5%	3
Si	ICP-ES	mg/kg	10	4.98E+02	14%	3	1.17E+03	2.6%	3	1.17E+03	2.6%	3
Sr	ICP-ES	mg/kg	10	2.73E+00	34%	3	7.24E+00	9.5%	3	7.24E+00	9.5%	3
Th	ICP-ES	mg/kg	11	4.75E+01	36%	3	*<1.0E+02*	--	3	4.75E+01	36%	3
Ti	ICP-ES	mg/kg	10	1.38E+01	34%	3	*<8.3E+01*	--	3	1.38E+01	34%	3
U	ICP-ES	mg/kg	20	1.26E+02	30%	3	*<3.8E+02*	--	3	1.26E+02	30%	3
Zn	ICP-ES	mg/kg	10	5.64E+00	36%	3	*<2.0E+01*	--	3	5.64E+00	36%	3
Zr	ICP-ES	mg/kg	11	9.06E+00	38%	3	--	--	--	9.06E+00	38%	3
Tc-99	ICP-MS	mg/kg	10	2.45E-01	14%	3	--	--	--	2.45E-01	14%	3
Cs-137	Cs-137	dpm/g	5	--	--	--	4.47E+07	22%	3	4.47E+07	22%	3
Th-232	ICP-MS	mg/kg	10	4.79E+01	31%	3	--	--	--	4.79E+01	31%	3
U-235	ICP-MS	mg/kg	10	9.45E-01	31%	3	--	--	--	9.45E-01	31%	3
U-236	ICP-MS	mg/kg	10	6.65E-02	34%	3	--	--	--	6.65E-02	34%	3
Np-237	ICP-MS	mg/kg	10	2.58E-01	32%	3	--	--	--	2.58E-01	32%	3
U-238	ICP-MS	mg/kg	10	1.50E+02	31%	3	--	--	--	1.50E+02	31%	3
Pu-239	ICP-MS	mg/kg	10	9.84E-01	31%	3	--	--	--	9.84E-01	31%	3
Pu-240	ICP-MS	mg/kg	10	9.45E-02	33%	3	--	--	--	9.45E-02	33%	3

Table A-2. Below Detection Limit Values for Digested Tank 22 Slurry (HTF-22-17-6).

analyte	method	units	Aqua regia	Peroxide fusion	Overall
Ag	ICP-ES	mg/kg	*<2.3E+00*	*<3.3E+01*	*<2.3E+00*
Be	ICP-ES	mg/kg	*<2.6E-01*	*<1.6E+00*	*<2.6E-01*
Co	ICP-ES	mg/kg	*<2.4E+00*	*<2.9E+01*	*<2.4E+00*
K	ICP-ES	mg/kg	*<4.4E+01*	*<5.2E+02*	*<4.4E+01*
Mo	ICP-ES	mg/kg	*<7.0E+00*	*<8.3E+01*	*<7.0E+00*
P	ICP-ES	mg/kg	*<3.7E+01*	*<3.7E+02*	*<3.7E+01*
Pb	ICP-ES	mg/kg	*<3.1E+01*	*<3.7E+02*	*<3.1E+01*
Sb	ICP-ES	mg/kg	*<3.3E+01*	*<3.9E+02*	*<3.3E+01*
Sn	ICP-ES	mg/kg	*<2.0E+01*	*<2.3E+02*	*<2.0E+01*
V	ICP-ES	mg/kg	*<9.1E-01*	*<1.3E+01*	*<9.1E-01*

Table A-3. Analytical Results of Tank 22 Supernate Composite Feed.

analyte	method	units	1σ (%)	Tank 22 supernate composite		
				average	RSD	*n*
density	gravimetric	g/mL		1.025	0.3%	2
OH^-	titration	M	10	1.89E-01	3.9%	4
NO_2^-	IC	mg/L	10	1.14E+04	10%	4
NO_3^-	IC	mg/L	10	4.00E+03	1.1%	4
CO_3^-	TIC/TOC	mg/L	10	2.83E+03	1.2%	4
SO_4^{2-}	IC	mg/L	10	6.05E+02	3.2%	4
$C_2O_4^{2-}$	IC	mg/L	10	2.25E+02	1.0%	4
TOC	TIC/TOC	mg C/L	10	1.03E+02	0.9%	4
TMS	SVOA	mg/L	20	2.20E+01	--	1
CH_3Hg^+	CGCVAFS	mg/L	20	2.29E+00	--	1
Al	ICP-ES	mg/L	15	1.40E+01	4.5%	4
B	ICP-ES	mg/L	10	4.85E+01	1.5%	4
Ca	ICP-ES	mg/L	10	5.77E-01	13%	4
Hg	CVAA	mg/L	20	1.71E+02	1.4%	4
Fe	ICP-ES	mg/L	10	2.22E+00	32%	4
K	ICP-ES	mg/L	20	2.97E+01	24%	4
Li	ICP-ES	mg/L	10	4.99E+01	1.3%	4
Mg	ICP-ES	mg/L	10	1.43E-01	28%	4
Mn	ICP-ES	mg/L	13	5.57E-01	34%	4
Na	ICP-ES	mg/L	10	1.36E+04	0.6%	4
S	ICP-ES	mg/L	30	3.11E+02	5.7%	4
Si	ICP-ES	mg/L	10	2.65E+02	1.0%	4
Tc-99	ICP-MS	mg/L	10	1.54E-01	0.7%	4
U-235	ICP-MS	mg/L	10	8.50E-03	4.6%	4
U-238	ICP-MS	mg/L	10	1.31E+00	5.1%	4

Table A-4. Below Detection Limit Values for Tank 22 Supernate Composite Feed.

analyte	method	units	Tk22 sup.	analyte	method	units	Tk22 sup.
F^-	IC	mg/L	*<1.0E+02*	Cu	ICP-ES	mg/L	*<1.1E+00*
CO_2H^-	IC	mg/L	*<1.0E+02*	Gd	ICP-ES	mg/L	*<7.0E-01*
Cl^-	IC	mg/L	*<1.0E+02*	La	ICP-ES	mg/L	*<2.3E-01*
PO_4^{3-}	IC	mg/L	*<1.0E+02*	Mo	ICP-ES	mg/L	*<1.7E+00*
Br^-	IC	mg/L	*<1.0E+02*	Ni	ICP-ES	mg/L	*<2.1E+00*
$C_2H_3O_3^{2-}$	IC	mg/L	*<1.0E+01*	P	ICP-ES	mg/L	*<1.0E+01*
HMDSO	SVOA	mg/L	*<1.0E-01*	Pb	ICP-ES	mg/L	*<4.2E+00*
propanal	VOA	mg/L	*<1.0E+00*	Sb	ICP-ES	mg/L	*<4.4E+00*
other SVOA	SVOA	mg/L	*<1.0E+00*	Sn	ICP-ES	mg/L	*<1.2E+01*
other VOA	VOA	mg/L	*<1.0E+00*	Sr	ICP-ES	mg/L	*<2.1E-01*
Ag	ICP-ES	mg/L	*<3.7E-01*	Th	ICP-ES	mg/L	*<2.0E+00*
Ba	ICP-ES	mg/L	*<1.7E-01*	Ti	ICP-ES	mg/L	*<1.8E+00*
Be	ICP-ES	mg/L	*<1.8E-01*	U	ICP-ES	mg/L	*<1.0E+01*
Cd	ICP-ES	mg/L	*<3.3E-01*	V	ICP-ES	mg/L	*<2.8E-01*
Ce	ICP-ES	mg/L	*<2.8E+00*	Zn	ICP-ES	mg/L	*<2.2E-01*
Co	ICP-ES	mg/L	*<4.5E-01*	Zr	ICP-ES	mg/L	*<1.4E-01*
Cr	ICP-ES	mg/L	*<3.7E-01*				

Table A-5. Analytical Results for the pH adjusted SC-18 SME Product Supernate used as the source of glycolate in Tank 22 HGR Test 3.

analyte	method	units	1σ (%)	adjusted SC-18 SME product		
				average	RSD	*n*
density	gravimetric	g/mL		1.12	--	1
OH^-	titration	M	10	3.11E-01	--	1
NO_2^-	IC	mg/L	10	1.26E+04	0.5%	3
NO_3^-	IC	mg/L	10	5.37E+04	0.4%	3
CO_3^{2-}	TIC/TOC	mg/L	10	1.43E+03	--	1
SO_4^{2-}	IC	mg/L	10	2.07E+03	1.2%	3
$C_2O_4^{2-}$	IC	mg/L	10	3.07E+03	7.9%	3
$C_2H_3O_3^{2-}$	IC	mg/L	10	3.50E+04	4.2%	3
TOC	TIC/TOC	mg C/L	10	6.92E+03	--	1
Al	ICP-ES	mg/L	10	2.09E+02	3.8%	3
B	ICP-ES	mg/L	10	2.10E+02	4.2%	3
Cr	ICP-ES	mg/L	10	3.91E+01	4.3%	3
Fe	ICP-ES	mg/L	10	1.44E+02	4.3%	3
K	ICP-ES	mg/L	11	8.63E+01	8.5%	3
Li	ICP-ES	mg/L	10	3.12E+02	3.6%	3
Mn	ICP-ES	mg/L	10	2.69E+01	4.6%	3
Na	ICP-ES	mg/L	10	5.55E+04	3.7%	3
S	ICP-ES	mg/L	16	9.12E+02	3.7%	3
Si	ICP-ES	mg/L	11	3.85E+01	2.2%	3
U	ICP-ES	mg/L	10	1.69E+02	5.8%	3
Zr	ICP-ES	mg/L	11	2.59E+00	3.7%	3
Tc-99	ICP-MS	mg/L	10	1.40E+00	3.1%	3
Th-232	ICP-MS	mg/L	10	6.06E-01	4.8%	3
U-233	ICP-MS	mg/L	10	2.95E-02	5.2%	3
U-234	ICP-MS	mg/L	10	3.90E-02	6.2%	3
U-235	ICP-MS	mg/L	10	1.73E+00	4.5%	3
U-236	ICP-MS	mg/L	10	1.00E-01	6.2%	3
Np-237	ICP-MS	mg/L	10	3.43E-01	5.3%	3
U-238	ICP-MS	mg/L	10	1.83E+02	4.6%	3
Pu-239	ICP-MS	mg/L	10	4.63E-02	5.7%	3

Two additional organic compounds were measured by SVOA at approximately 8 mg/L each.

Table A-6. Below Detection Limit Values for the pH adjusted SC-18 SME Product Supernate used as the source of glycolate in Tank 22 HGR Test 3.

analyte	method	units	result
Cl^-	IC	mg/L	*<1.0E+01*
PO_4^{3-}	IC	mg/L	*<1.0E+01*
Ag	ICP-ES	mg/L	*<9.0E-01*
Ba	ICP-ES	mg/L	*<2.2E-01*
Be	ICP-ES	mg/L	*<4.7E-02*
Ca	ICP-ES	mg/L	*<7.3E-01*
Cd	ICP-ES	mg/L	*<8.9E-01*
Ce	ICP-ES	mg/L	*<2.4E+00*
Co	ICP-ES	mg/L	*<9.7E-01*
Cu	ICP-ES	mg/L	*<3.2E+00*
Gd	ICP-ES	mg/L	*<7.8E-01*
Hg	CVAA	mg/L	*<1.2E+00*
La	ICP-ES	mg/L	*<6.9E-01*
Mg	ICP-ES	mg/L	*<1.4E-01*
Mo	ICP-ES	mg/L	*<2.8E+00*
Ni	ICP-ES	mg/L	*<1.5E+00*
P	ICP-ES	mg/L	*<1.2E+01*
Pb	ICP-ES	mg/L	*<1.2E+01*
Sb	ICP-ES	mg/L	*<1.3E+01*
Sn	ICP-ES	mg/L	*<7.7E+00*
Sr	ICP-ES	mg/L	*<1.3E-01*
Th	ICP-ES	mg/L	*<4.2E+00*
Ti	ICP-ES	mg/L	*<2.7E+00*
V	ICP-ES	mg/L	*<4.1E-01*
Zn	ICP-ES	mg/L	*<3.5E-01*

Table A-7. Analytical Results of Post-HGR Tank 22 Supernate.

analyte	method	units	1σ (%)	Test 1			Test 2			Test 3			Test 4		
				average	RSD	*n*	average	RSD	*n*	average	RSD	*n*	average	RSD	*n*
density	gravimetric	g/mL		1.026	0.1%	2	1.028	0.1%	2	1.029	0.1%	2	1.034	1.3%	5
F^-	IC	mg/L	10	*<1.0E+02*	--	2	*<1.0E+02*	--	2	3.53E+01	0.4%	3	*<1.0E+02*	--	2
CHO_2^-	IC	mg/L	10	*<1.0E+02*	--	2	*<1.0E+02*	--	2	1.09E+02	0.5%	3	*<1.0E+02*	--	2
Cl^-	IC	mg/L	10	*<1.0E+02*	--	2	*<1.0E+02*	--	2	1.67E+01	0.6%	3	*<1.0E+02*	--	2
NO_2^-	IC	mg/L	10	1.19E+04	1.2%	2	1.16E+04	3.7%	2	1.15E+04	0.5%	3	1.17E+04	1.8%	2
NO_3^-	IC	mg/L	10	3.64E+03	12.0%	2	4.74E+03	13.0%	2	4.35E+03	0.1%	3	4.77E+03	1.3%	2
SO_4^{2-}	IC	mg/L	10	5.98E+02	5.1%	2	6.55E+02	3.3%	2	6.23E+02	0.5%	3	5.52E+02	1.4%	2
$C_2O_4^{2-}$	IC	mg/L	10	1.96E+02	1.1%	2	2.02E+02	1.8%	2	2.45E+02	0.5%	3	2.03E+02	0.7%	2
$C_2H_3O_3^{2-}$	IC	mg/L	10	*<1.0E+01*	--	2	1.32E+02	1.6%	2	1.75E+02	2.0%	3	1.42E+02	1.5%	2
OH^-	titration	M	10	1.71E-01	2.5%	2	1.89E-01	1.1%	3	1.84E-01	--	1	1.92E-01	--	1
CO_3^{2-}	TIC/TOC	mg/L	10	2.54E+03	2.2%	2	2.53E+03	0.5%	3	2.56E+03	--	1	2.46E+03	--	1
TOC	TIC/TOC	mg C/L	10	*<2.0E+01*	--	2	4.28E+01	6.1%	3	6.16E+01	--	1	3.91E+01	--	1
CH_3Hg^+	GCCVAFS	mg/L	20	2.40E+00	--	1	--	--	0	--	--	0	2.55E+00	--	1
Al	ICP-ES	mg/L	10	1.17E+01	3.0%	2	1.18E+01	0.6%	2	1.24E+01	2.8%	3	6.59E+01	0.6%	3
B	ICP-ES	mg/L	10	4.17E+01	2.0%	2	4.10E+01	0.0%	2	4.45E+01	0.8%	3	4.07E+01	0.8%	3
Fe	ICP-ES	mg/L	11	*<4.1E-01*	--	2	*<4.1E-01*	--	2	4.74E-01	2.2%	3	*<4.1E-01*	--	3
Hg	CVAA	mg/L	20	2.25E+02	--	1	2.17E+02	--	1	2.21E+02	--	1	3.65E+02	--	1
K	ICP-ES	mg/L	15	3.24E+01	3.1%	2	2.51E+01	2.3%	2	2.80E+01	6.9%	3	2.86E+01	--	1
Li	ICP-ES	mg/L	10	4.79E+01	1.3%	2	4.73E+01	0.3%	2	5.02E+01	0.6%	3	4.34E+01	0.9%	3
Na	ICP-ES	mg/L	10	1.34E+04	2.6%	2	1.37E+04	2.6%	2	1.43E+04	4.3%	3	1.34E+04	1.1%	3
P	ICP-ES	mg/L	20	5.74E+00	2.7%	2	5.25E+00	1.8%	2	5.57E+00	3.4%	3	*<1.8E+01*	--	3
Si	ICP-ES	mg/L	10	2.34E+02	1.2%	2	2.34E+02	0.3%	2	2.40E+02	0.6%	3	1.97E+02	0.3%	3

Table A-8. Below Detection Limit Values for Post-HGR Tank 22 Supernate.

analyte	method	units	Test 1	Test 2	Test 3	Test 4
PO_4^{3-}	IC	mg/L	*<1.0E+02*	*<1.0E+02*	*<1.0E+01*	*<1.0E+02*
Br^-	IC	mg/L	*<1.0E+02*	*<1.0E+02*	*<1.0E+02*	*<1.0E+02*
Ag	ICP-ES	mg/L	*<3.1E-01*	*<3.1E-01*	*<3.1E-01*	*<3.1E-01*
Ba	ICP-ES	mg/L	*<7.6E-02*	*<7.6E-02*	*<7.6E-02*	*<7.6E-02*
Be	ICP-ES	mg/L	*<4.8E-02*	*<1.8E-02*	*<1.8E-02*	*<1.8E-02*
Ca	ICP-ES	mg/L	*<2.5E-01*	*<2.5E-01*	*<2.5E-01*	*<3.9E-01*
Cd	ICP-ES	mg/L	*<3.0E-01*	*<3.0E-01*	*<3.0E-01*	*<3.0E-01*
Ce	ICP-ES	mg/L	*<8.0E-01*	*<8.0E-01*	*<8.0E-01*	*<8.0E-01*
Co	ICP-ES	mg/L	*<3.3E-01*	*<3.3E-01*	*<3.3E-01*	*<3.3E-01*
Cr	ICP-ES	mg/L	*<1.7E-01*	*<1.7E-01*	*<1.7E-01*	*<1.7E-01*
Cu	ICP-ES	mg/L	*<1.1E+00*	*<1.1E+00*	*<1.1E+00*	*<1.1E+00*
Gd	ICP-ES	mg/L	*<2.3E-01*	*<2.3E-01*	*<2.3E-01*	*<2.3E-01*
La	ICP-ES	mg/L	*<2.3E-01*	*<2.3E-01*	*<2.3E-01*	*<2.3E-01*
Mg	ICP-ES	mg/L	*<4.3E-02*	*<4.3E-02*	*<4.3E-02*	*<4.3E-02*
Mn	ICP-ES	mg/L	*<4.2E-02*	*<4.2E-02*	*<4.2E-02*	*<4.2E-02*
Mo	ICP-ES	mg/L	*<9.3E-01*	*<9.3E-01*	*<9.3E-01*	*<9.3E-01*
Ni	ICP-ES	mg/L	*<1.2E+00*	*<1.2E+00*	*<1.2E+00*	*<1.2E+00*
Pb	ICP-ES	mg/L	*<4.2E+00*	*<4.2E+00*	*<4.2E+00*	*<4.2E+00*
S	ICP-ES	mg/L	*<2.6E+02*	*<3.0E+02*	*<2.6E+02*	*<2.6E+02*
Sb	ICP-ES	mg/L	*<4.4E+00*	*<4.4E+00*	*<4.4E+00*	*<4.4E+00*
Sn	ICP-ES	mg/L	*<2.6E+00*	*<2.6E+00*	*<2.6E+00*	*<2.6E+00*
Sr	ICP-ES	mg/L	*<2.1E-02*	*<2.1E-02*	*<2.1E-02*	*<2.1E-02*
Th	ICP-ES	mg/L	*<1.1E+00*	*<1.1E+00*	*<1.1E+00*	*<1.1E+00*
Ti	ICP-ES	mg/L	*<9.3E-01*	*<9.3E-01*	*<9.3E-01*	*<9.3E-01*
U	ICP-ES	mg/L	*<4.3E+00*	*<4.3E+00*	*<4.3E+00*	*<4.3E+00*
V	ICP-ES	mg/L	*<2.8E-01*	*<2.8E-01*	*<2.8E-01*	*<2.8E-01*
Zn	ICP-ES	mg/L	*<2.2E-01*	*<2.2E-01*	*<2.2E-01*	*<2.2E-01*
Zr	ICP-ES	mg/L	*<1.4E-01*	*<1.4E-01*	*<1.4E-01*	*<1.4E-01*

Appendix B. Hydrogen Generation Rate Test Plots

Please see Section 3.1.1 for an explanation of these plots, including limitations of these data.

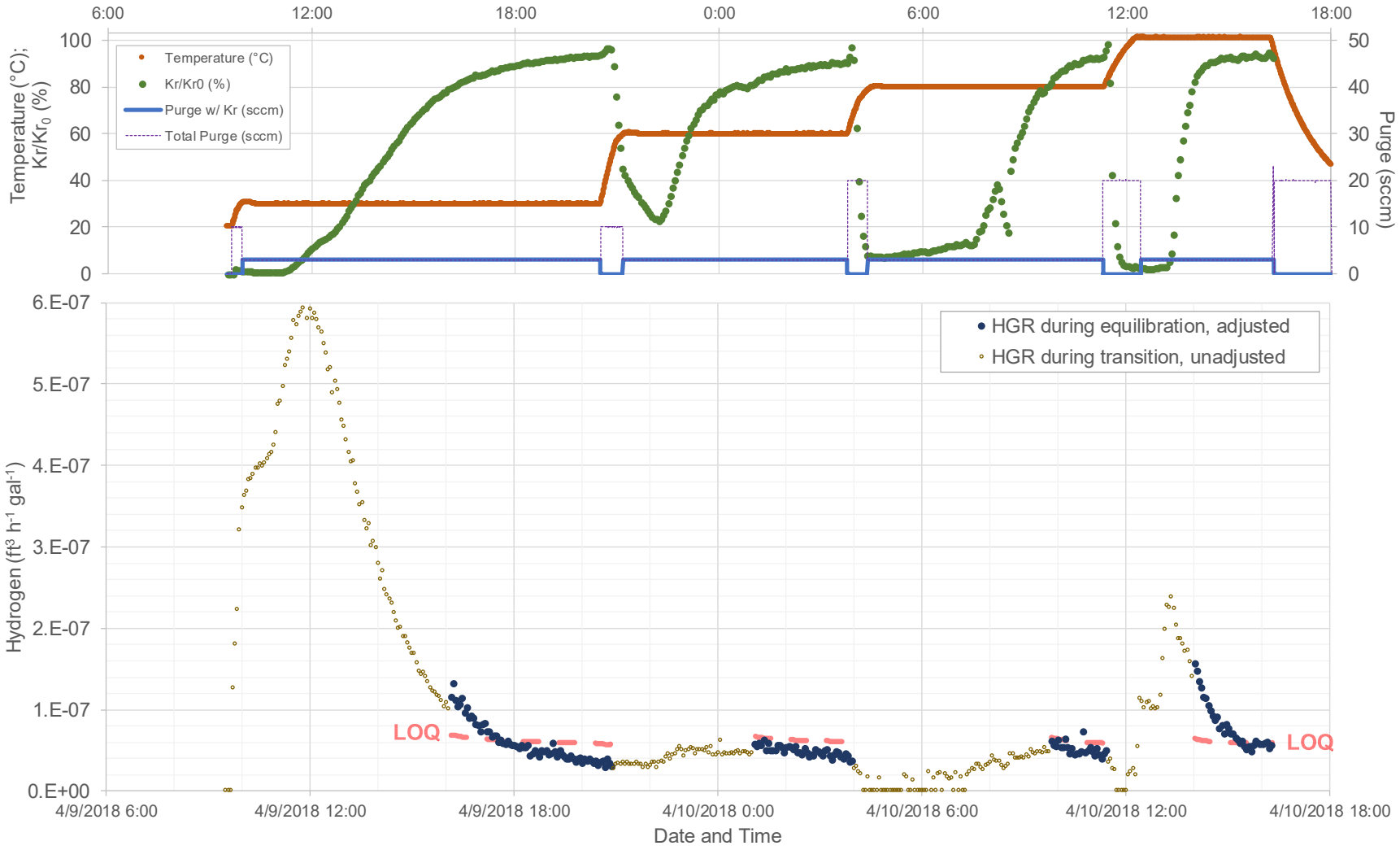

Figure B-1. Test 1: Tank 22 sample supernate with no glycolate added.

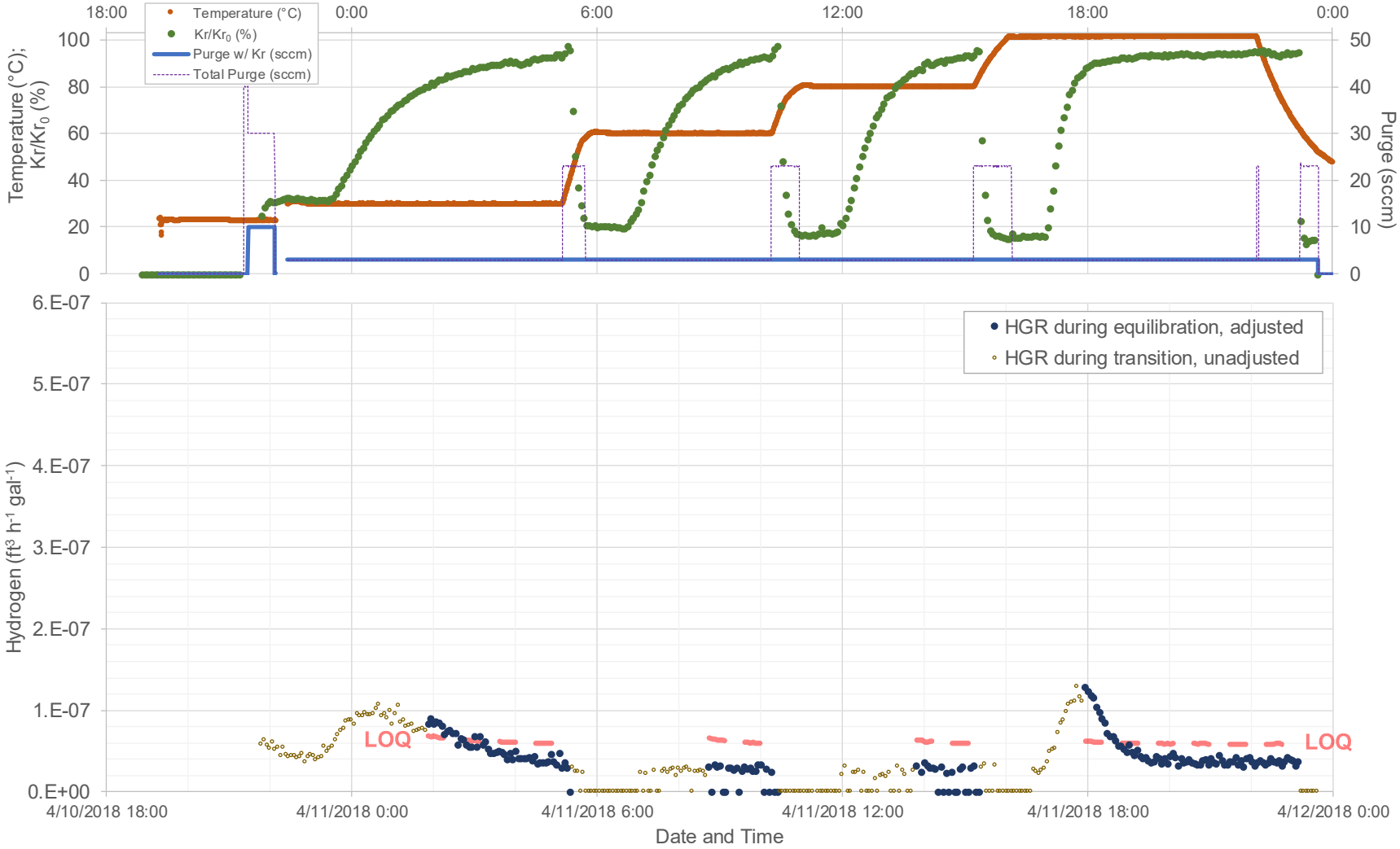

Figure B-2. Test 2: Tank 22 sample supernate with 120 mg/L glycolate added as sodium glycolate.

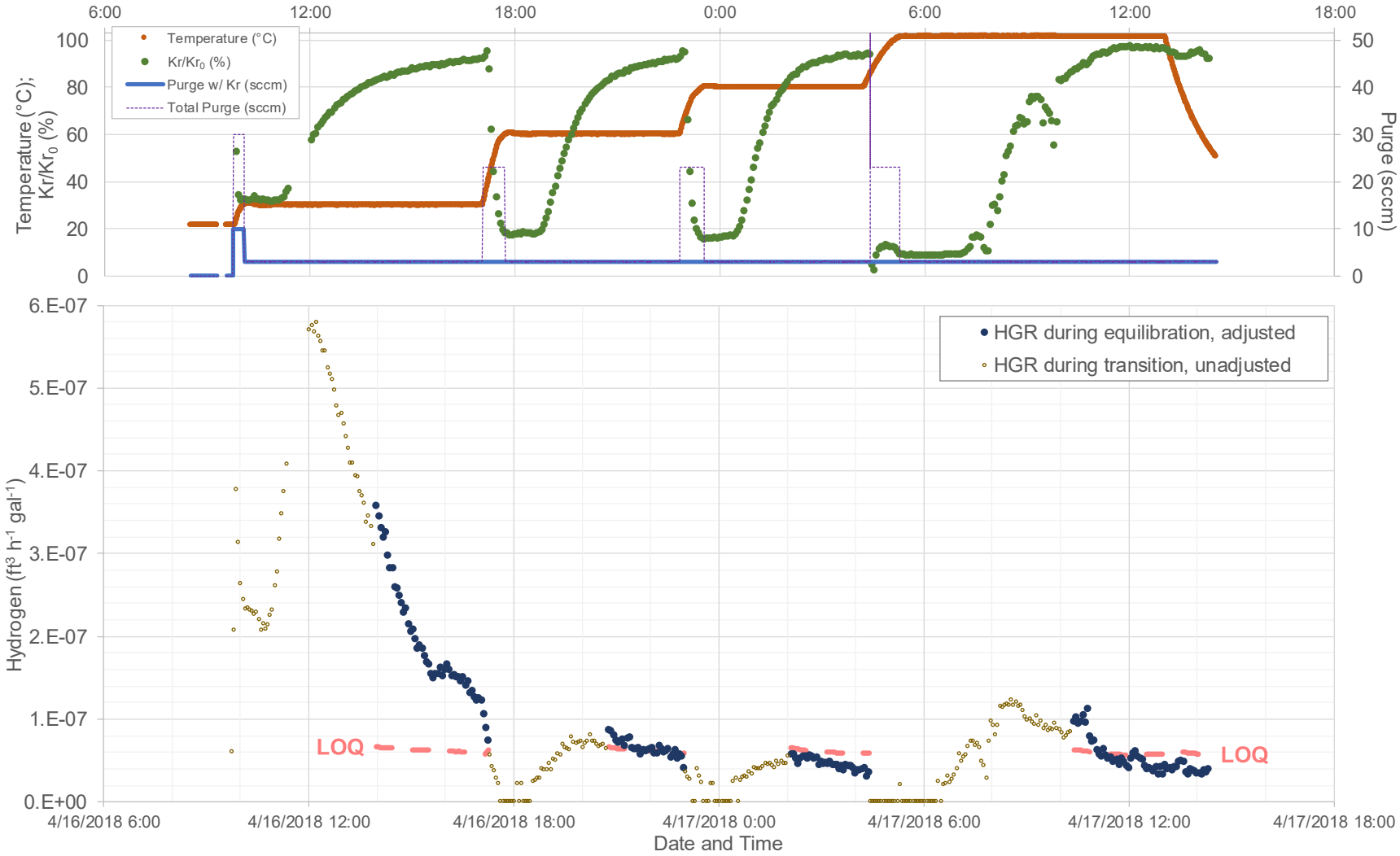

Figure B-3. Test 3: Tank 22 sample supernate with 120 mg/L glycolate added as adjusted SC-18 SME product.

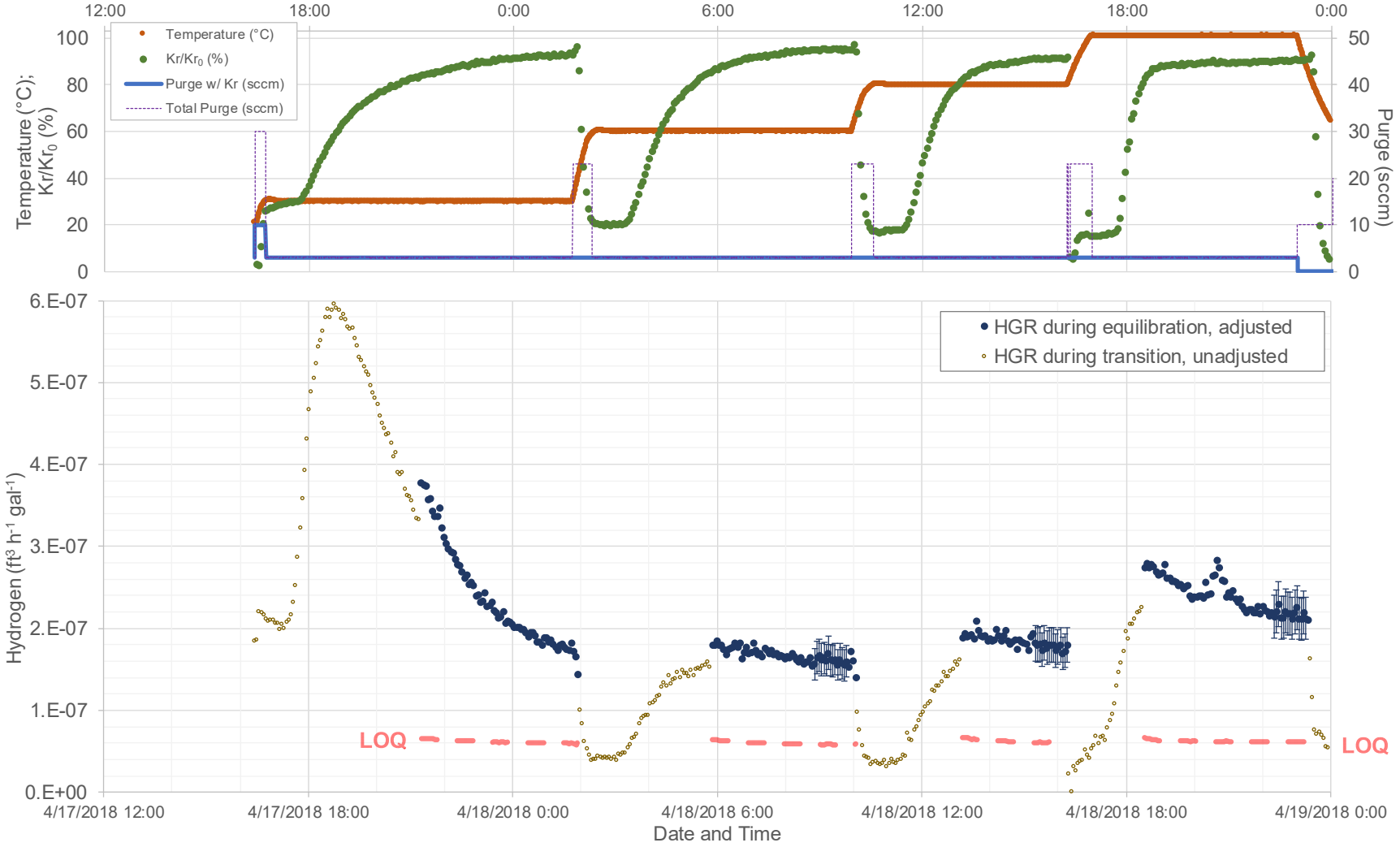

Figure B-4. Test 4: Tank 22 sample slurry with 120 mg/L glycolate added as sodium glycolate.

Distribution:

timothy.brown@srnl.doe.gov
alex.cozzi@srnl.doe.gov
david.crowley@srnl.doe.gov
David.Dooley@srnl.doe.gov
a.fellinger@srnl.doe.gov
samuel.fink@srnl.doe.gov
nancy.halverson@srnl.doe.gov
erich.hansen@srnl.doe.gov
connie.herman@srnl.doe.gov
david.herman@srnl.doe.gov
Kevin.Fox@srnl.doe.gov
john.mayer@srnl.doe.gov
daniel.mccabe@srnl.doe.gov
Gregg.Morgan@srnl.doe.gov
frank.pennebaker@srnl.doe.gov
William.Ramsey@SRNL.DOE.gov
luke.reid@srnl.doe.gov
geoffrey.smoland@srnl.doe.gov
michael.stone@srnl.doe.gov
Boyd.Wiedenman@srnl.doe.gov
bill.wilmarth@srnl.doe.gov
Records Administration (EDWS)
jeffrey.crenshaw@srs.gov
james.folk@srs.gov
roberto.gonzalez@srs.gov
tony.polk@srs.gov
jean.ridley@srs.gov
patricia.suggs@srs.gov
chris.martino@srnl.doe.gov
john.pareizs@srnl.doe.gov
david.newell@srnl.doe.gov
charles.crawford@srnl.doe.gov
Kevin.Brotherton@srs.gov
Richard.Edwards@srs.gov
terri.fellinger@srs.gov
eric.freed@srs.gov
jeffrey.gillam@srs.gov
barbara.hamm@srs.gov
bill.holtzscheiter@srs.gov
john.iaukea@srs.gov
Vijay.Jain@srs.gov
Victoria.Kmiec@srs.gov
jeff.ray@srs.gov
paul.ryan@srs.gov
Azadeh.Samadi-Dezfouli@srs.gov
hasmukh.shah@srs.gov
aaron.staub@srs.gov
celia.aponte@srs.gov
timothy.baughman@srs.gov
earl.brass@srs.gov
Thomas.Huff@srs.gov
Christine.Ridgeway@srs.gov
Christie.sudduth@srs.gov
arthur.wiggins@srs.gov
thomas.colleran@srs.gov
MARIA.RIOS-ARMSTRONG@SRS.GOV
Mason.Clark@srs.gov
Grace.Chen@srs.gov
john.occhipinti@srs.gov
Jocelin.Stevens@srs.gov
ryan.mcnew@srs.gov